ESI

Tin(IV) fluoride complexes with neutral phosphine coordination and comparisons with hard N- and O-donor ligands

Rhys P. King[a], Madeleine S. Woodward[a], Julian Grigg[b], Graeme McRobbie[b], William Levason[a] and Gillian Reid[a]*

Table S1 X-ray crystallographic data.[a]

Compound	$[SnF_3(PMe_3)_2(OTf)]$	$[Sn(PMe_3)_2(OTf)_2]$	$Sn_3F_5(OTf)$	$[SnF_4(\kappa^2\text{-triphos})]$
Formula	$C_7H_{18}F_6O_3P_2SSn$	$C_8H_{18}F_6O_6P_2S_2Sn$	$CF_8O_3SSn_3$	$C_{41}H_{39}F_4P_3Sn$
M	476.90	568.97	600.14	819.32
Crystal system	Orthorhombic	Monoclinic	Monoclinic	Monoclinic
Space group (no.)	Pbca (61)	$P2_1/n$ (14)	$P2_1/n$ (14)	$P2_1/n$ (14)
a /Å	11.4007(2)	12.9043(3)	13.4971(4)	13.8624(2)
b /Å	11.84650(10)	10.9889(3)	7.6953(2)	12.9086(2)
c /Å	23.9749(3)	15.1867(6)	10.7894(30	20.5379(4)
α /°	90	90	90	90
β /°	90	110.338(3)	97.810(2)	98.7350(17)
γ /°	90	90	90	90
U /Å^3	3238.01(7)	2019.27(11)	1110.24(5)	3632.50(11)
Z	8	4	4	4
μ(Mo-K_α) /mm^{-1}	1.967	1.704	6.983	0.886
F(000)	1872	1120	1072	1664
Total number reflns	85205	15141	29342	59518
R_{int}	0.079	0.044	0.122	0.044
Unique reflns	5553	6008	3642	11707
No. of params, restraints	187, 0	232, 0	145, 0	443, 0
GOF	1.014	1.052	1.030	1.035
R_1, wR_2 [$I > 2\sigma(I)$][b]	0.0236, 0.0518	0.043, 0.098	0.036, 0.075	0.033, 0.072
R_1, wR_2 (all data)	0.0305, 0.0546	0.061, 0.103	0.052, 0.080	0.048, 0.077

[a] common data: T = 100 K; wavelength (Mo-K_α) = 0.71073 Å; θ(max) = 27.5° ; [b] $R_1 = \Sigma||F_o| - |F_c||/\Sigma|F_o|$; $wR_2 = [\Sigma w(F_o^2 - F_c^2)^2/\Sigma wF_o^4]^{1/2}$.

Table S1 cont.

Compound	$[SnF_4(pyNO)_2]\cdot CH_2Cl_2$	$[SnF_4(py)_2]$	$[SnF_2(OPPh_3)_4][OTf]_2$
Formula	$C_{22}H_{24}Cl_4F_8N_4O_4Sn_2$	$C_{10}H_{10}F_4N_2Sn$	$C_{74}H_{60}F_8O_{10}P_4S_2Sn$
M	469.82	342.81	1567.91
Crystal system	Triclinic	Triclinic	Triclinic
Space group (no.)	P-1 (2)	P-1 (2)	P-1 (2)
a /Å	9.4615(3)	6.3696(4)	13.7031(3)
b /Å	11.2482(3)	7.2222(4)	15.6126(4)
c /Å	15.4968(5)	7.2263(3)	18.1412(4)
α /°	90.899(3)	117.933(5)	69.740(2)
β /°	103.213(3)	91.612(4)	70.468(2
γ /°	101.930(3)	109.045(5)	76.875(2)
U /Å^3	1567.47(9)	271.02(3)	3404.20(15)
Z	4	1	2
μ(Mo-K_α) /mm^{-1}	2.019	2.387	0.613
F(000)	911.269	160	1596
Total number reflns	20963	6755	80126
R_{int}	0.0769	0.043	0.0499
Unique reflns	7617	1396	17545
No. of params, restraints	397, 0	79, 0	892, 0
GOF	1.0361	1.182	1.020
R_1, wR_2 [$I > 2\sigma(I)$][b]	0.0552, 0.1560	0.067, 0.211	0.0469, 0.1160
R_1, wR_2 (all data)	0.0675, 0.1635	0.067, 0.211	0.0663, 0.1301

Spectroscopic data

Figure S1 [$SnF_4(P^iPr_3)_2$]

Figure S1.1 ^1H NMR spectrum (CD_2Cl_2, 298 K) (CH_2Cl_2[%]):

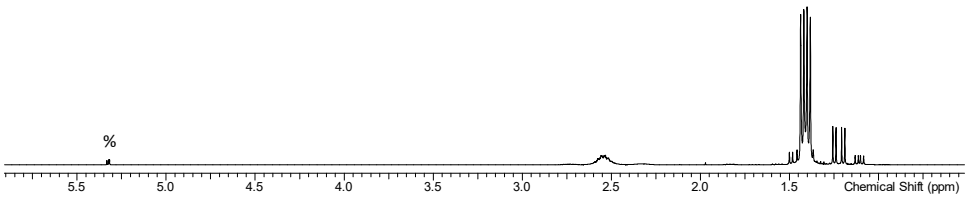

Figure S1.2 $^{19}F\{^1H\}$ NMR spectrum (CD_2Cl_2, 298 K):

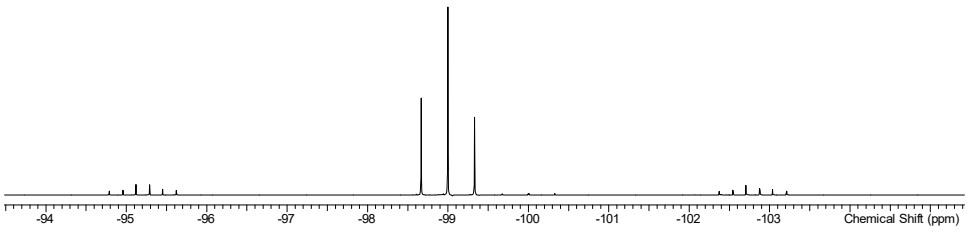

Figure S1.3 $^{31}P\{^1H\}$ NMR spectrum (CH_2Cl_2, 298 K):

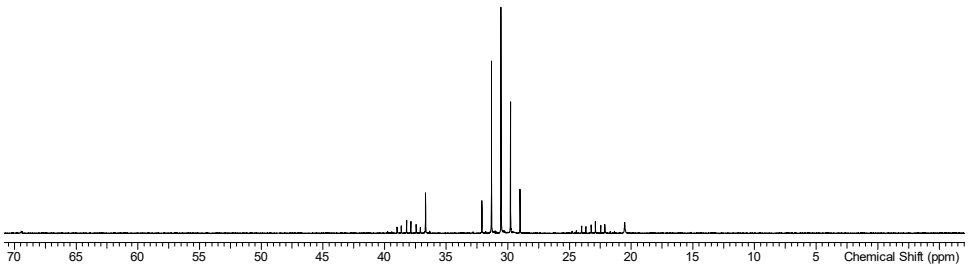

Figure S1.4 ^{119}Sn NMR spectrum (CD_2Cl_2, 183 K):

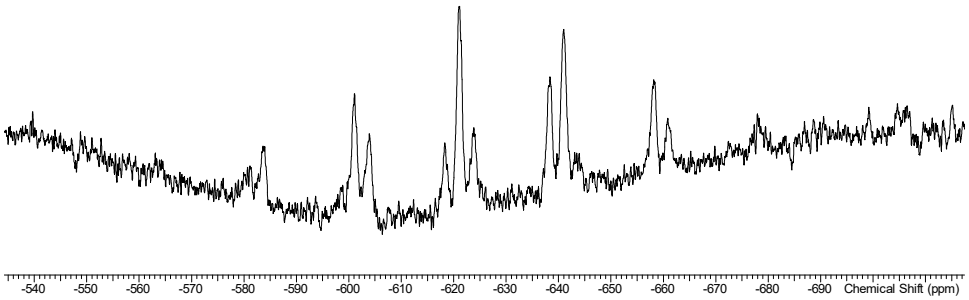

Figure S1.5 IR spectrum (Nujol/cm^{-1}):

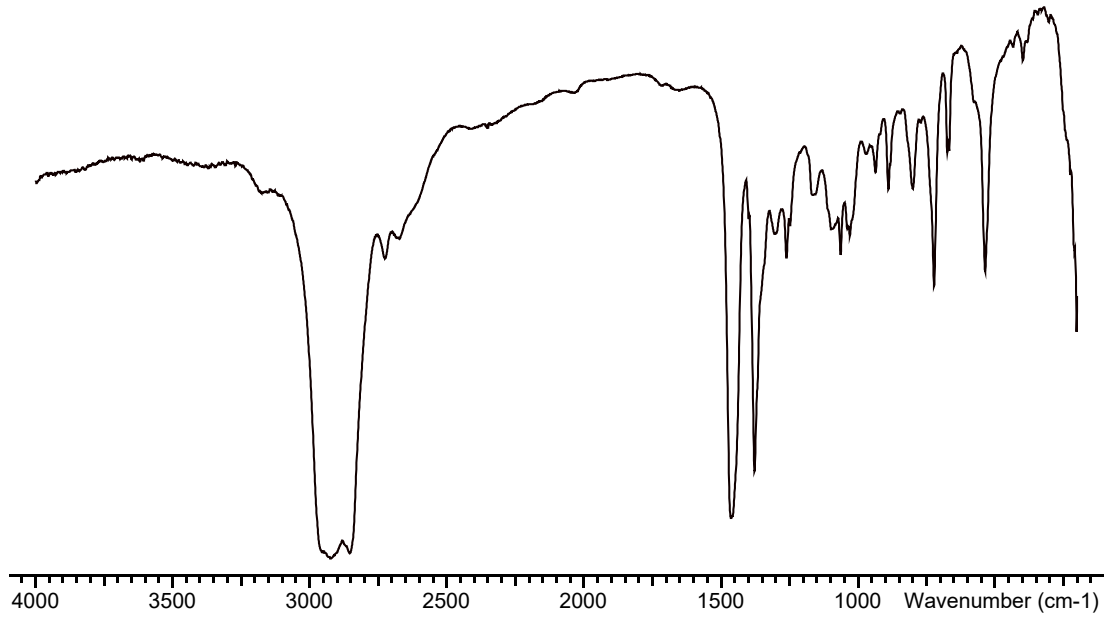

Figure S2. [$SnF_3(PMe_3)_2(OTf)$]

Figure S2.1 ^{1}H NMR spectrum (CD_2Cl_2, 298 K) (* = $[HPMe_3]^+$ impurity, CH_2Cl_2%):

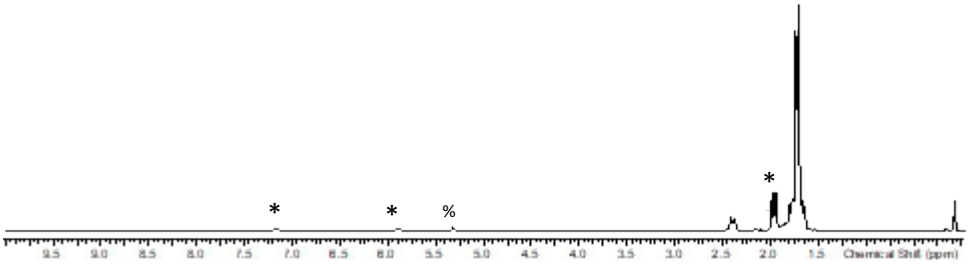

Figure S2.2.1 $^{19}F\{^{1}H\}$ NMR spectrum (CD_2Cl_2, 298 K):

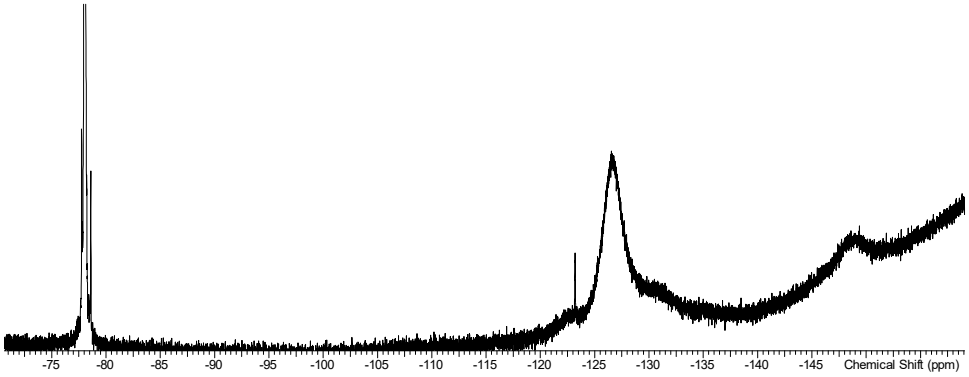

Figure S2.2.2 $^{19}F\{^{1}H\}$ NMR spectrum in CD_2Cl_2 (CD_2Cl_2, 183 K):

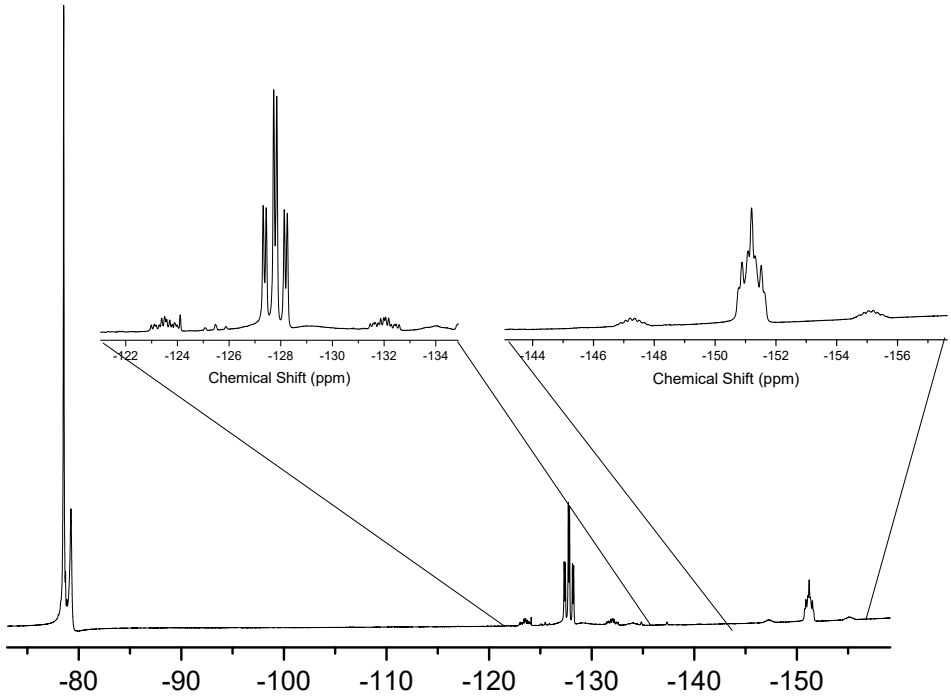

Figure S2.3.1 $^{31}P\{^{1}H\}$ NMR spectrum (CH_2Cl_2, 298 K) (* = $[HPMe_3]^+$ impurity)::

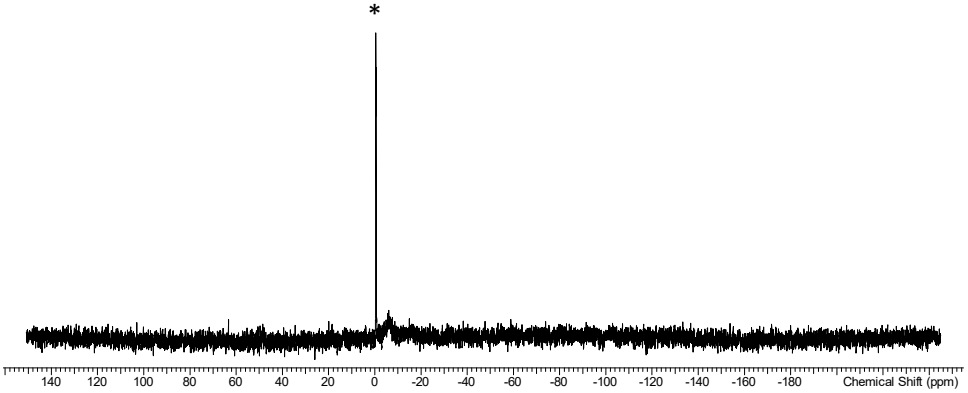

Figure S2.3.2 $^{31}P\{^{1}H\}$ NMR spectrum (CH_2Cl_2, 183 K) (* = $[HPMe_3]^+$ impurity):

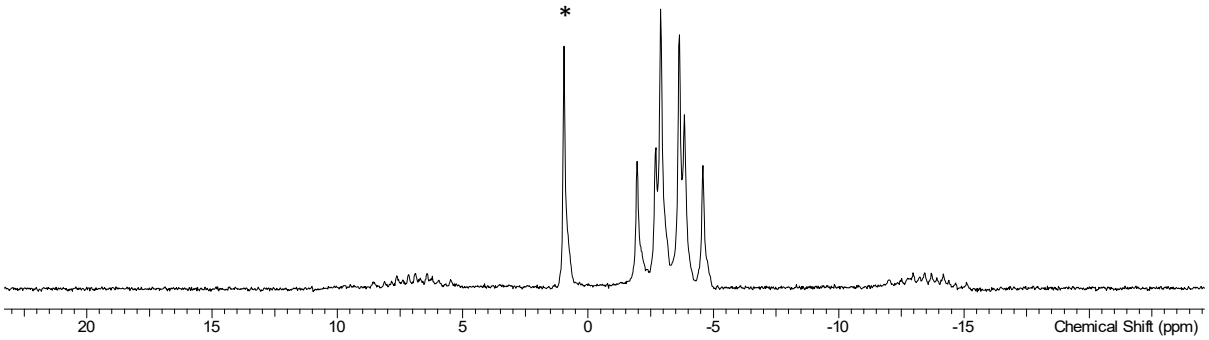

Figure S2.4 ^{119}Sn NMR spectrum (CH_2Cl_2, 183 K):

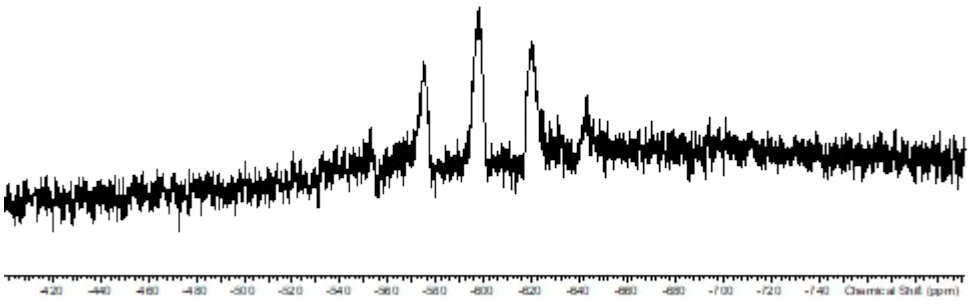

Figure S2.5 IR spectrum (Nujol/cm^{-1}):

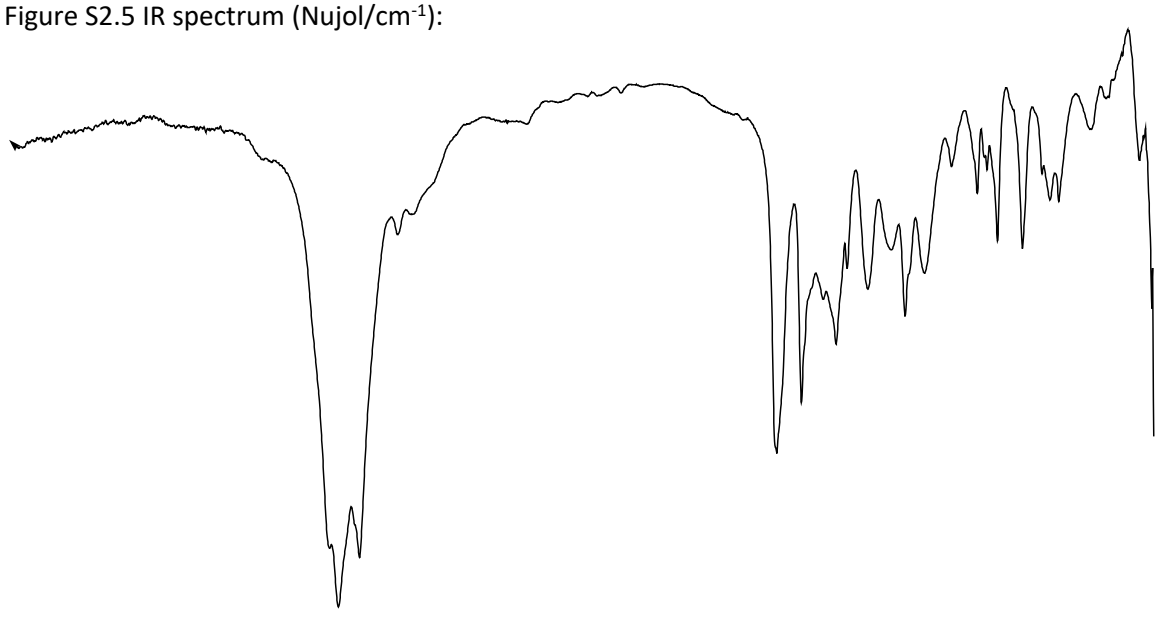

Figure S3 [$SnF_2(PMe_3)_2(OTf)_2$]

Figure S3.1 ^{1}H NMR spectrum (CD_2Cl_2, 298 K) (* $[HPMe_3]^+$ impurity, CH_2Cl_2%):

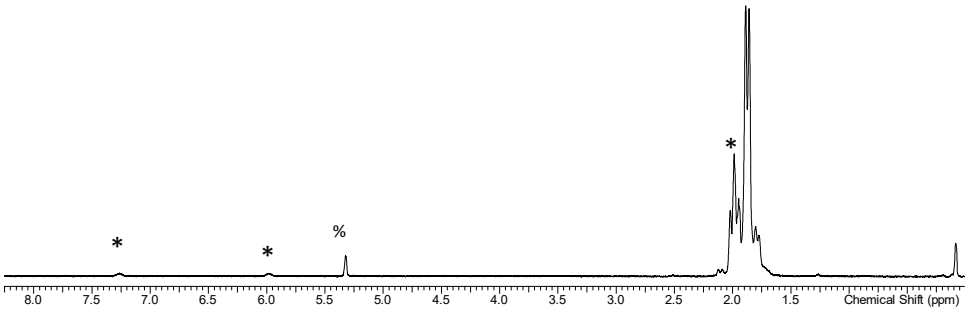

Figure S3.2.1 $^{19}F\{^{1}H\}$ NMR spectrum (CD_2Cl_2, 298 K):

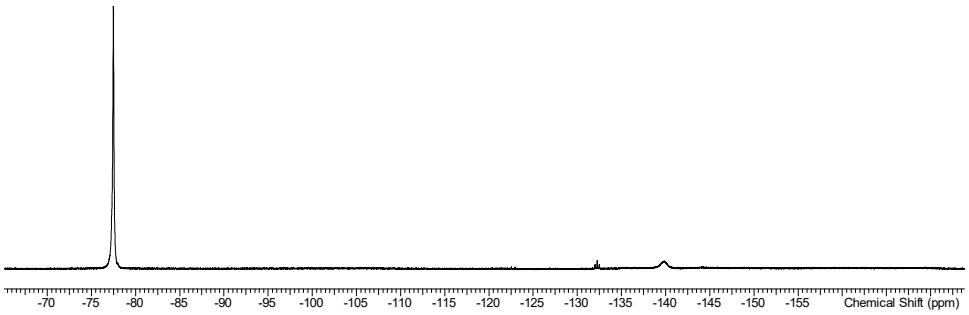

Figure S3.2.2 $^{19}F\{^{1}H\}$ NMR spectrum (CD_2Cl_2, 183 K):

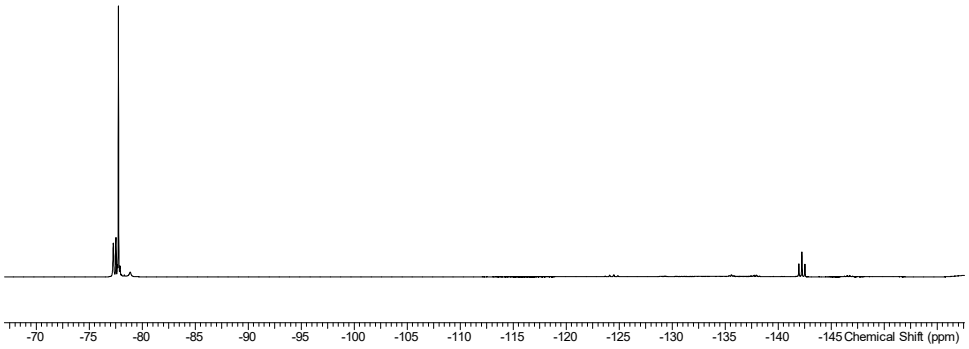

Figure S3.2.3 Expansion of multiplet at -142.7 ppm:

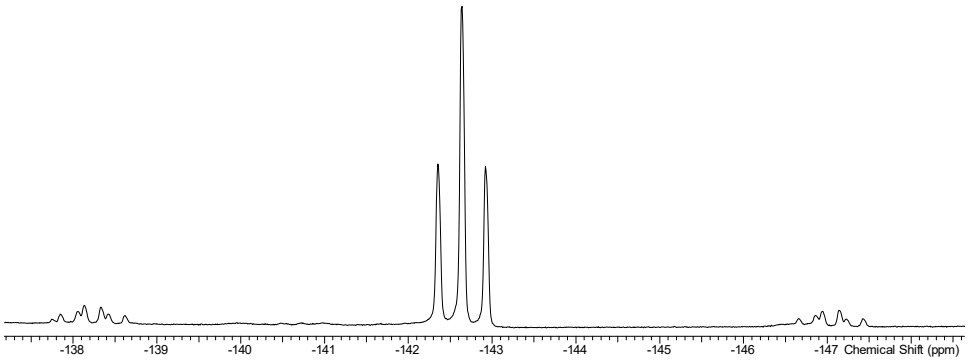

Figure S3.3.1 $^{31}P\{^{1}H\}$ NMR spectrum (CH_2Cl_2, 298 K):

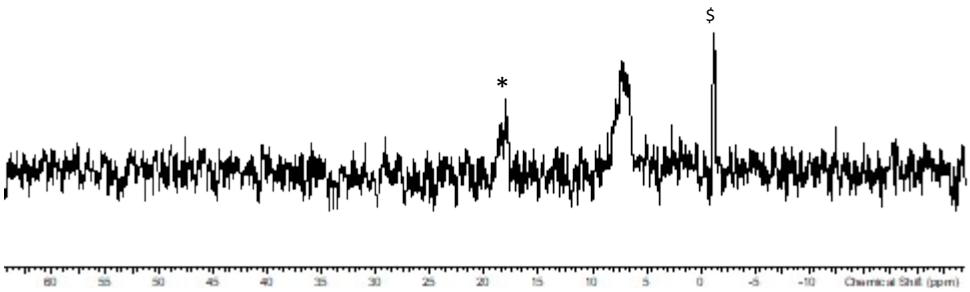

Figure S3.3.2 $^{31}P\{^{1}H\}$ NMR spectrum (CH_2Cl_2, 183 K) (* $[SnF(PMe_3)_2(OTf)_3]$ impurity. $ $[HPMe_3]^+$ impurity,

+ unidentified impurity)

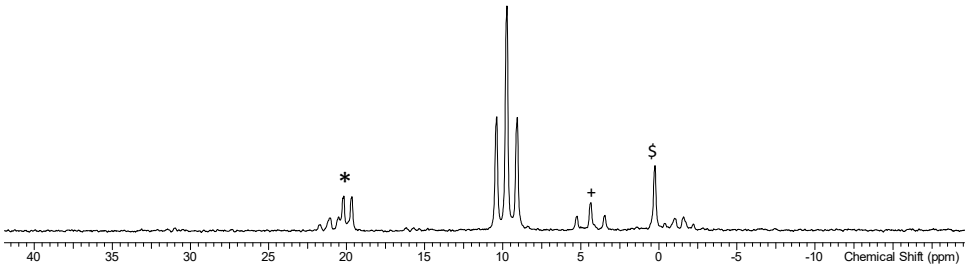

Figure S3.4 ^{119}Sn NMR spectrum (CH_2Cl_2, 183 K):

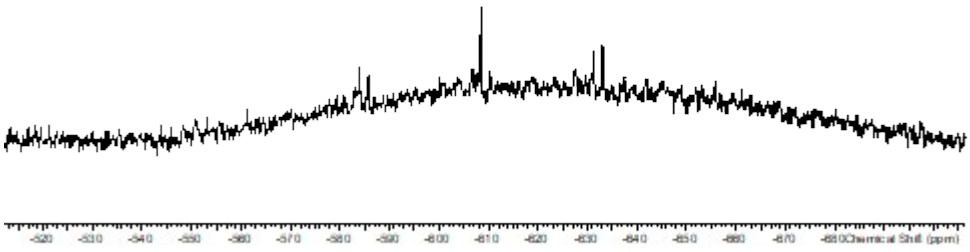

Figure S3.5 IR spectrum (Nujol/cm^{-1}):

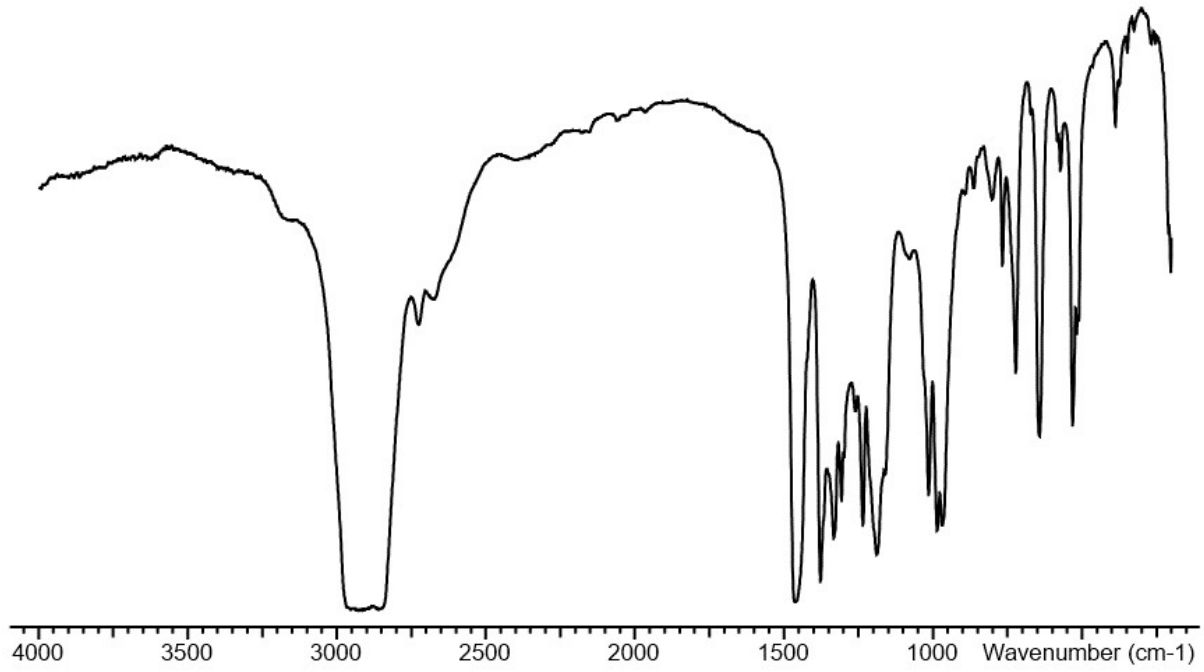

Figure S4 [SnF(PMe$_3$)$_2$(OTf)$_3$]

Figure S4.1.1 ^{1}H NMR spectrum *in situ* (CD_2Cl_2, 298 K) (* = $FSiMe_3$, CH_2Cl_2[%]):

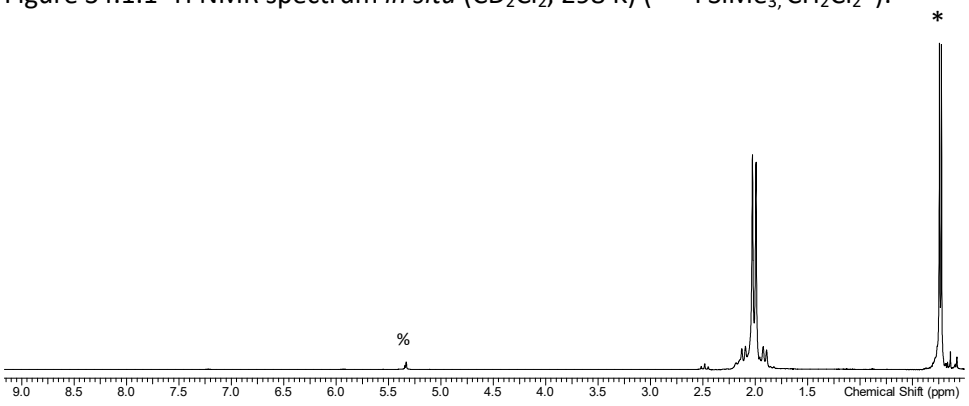

Figure S4.1.2 ^{1}H NMR spectrum immediately on isolation (CD_2Cl_2, 298 K) (*[$FPMe_3$]$^+$, $ decomposition, CH_2Cl_2[%]):

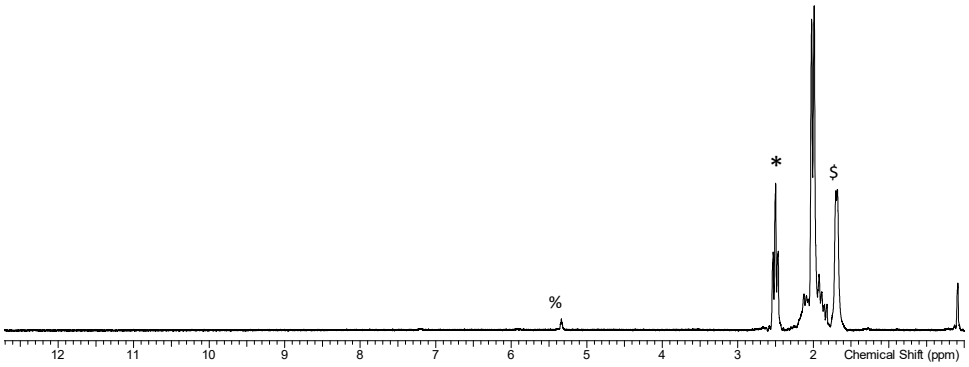

Figure S4.2.1 $^{19}F\{^{1}H\}$ NMR spectrum of isolated product (CD_2Cl_2, 298 K) (* = $[PMe_3F]^+$ impurity):

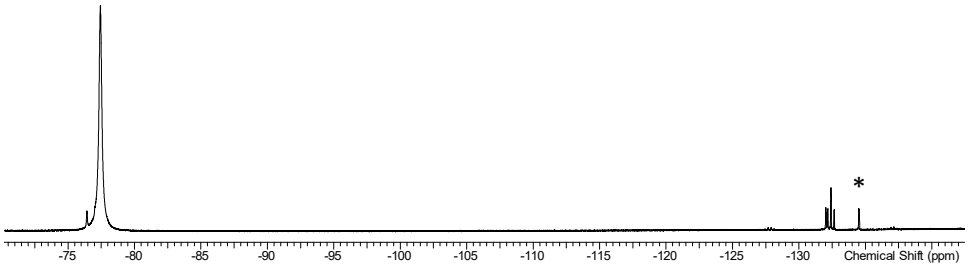

Figure S4.2.2 Zoomed in picture of isolated product multiplet

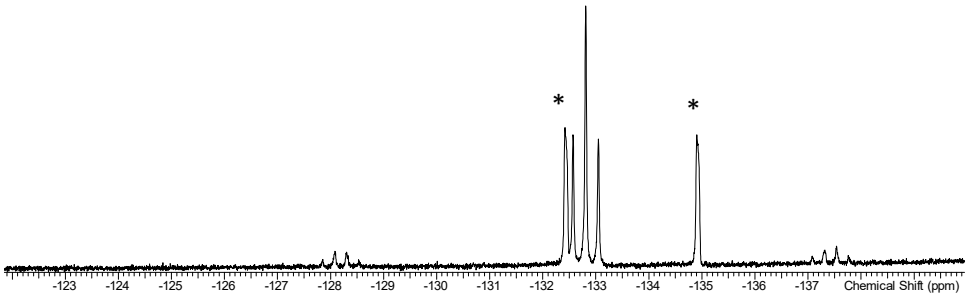

Figure S4.3.1 $^{19}F\{^{1}H\}$ in situ: $*FSiMe_3$

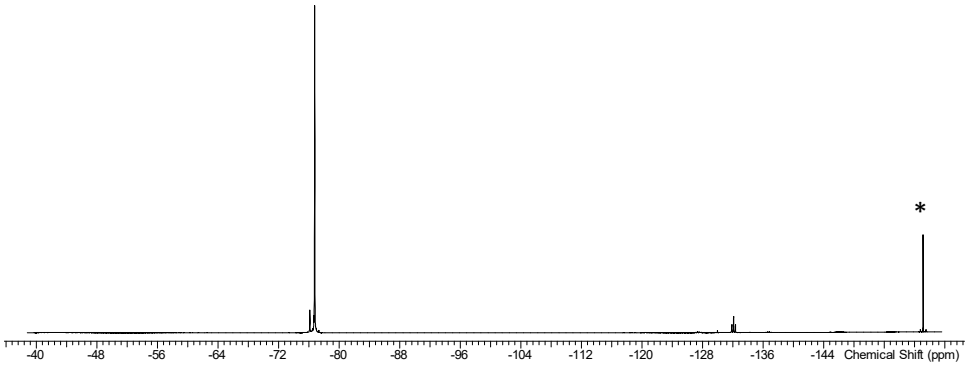

Figure S4.3.2 Expansion of the multiplet at -132.9 ppm:

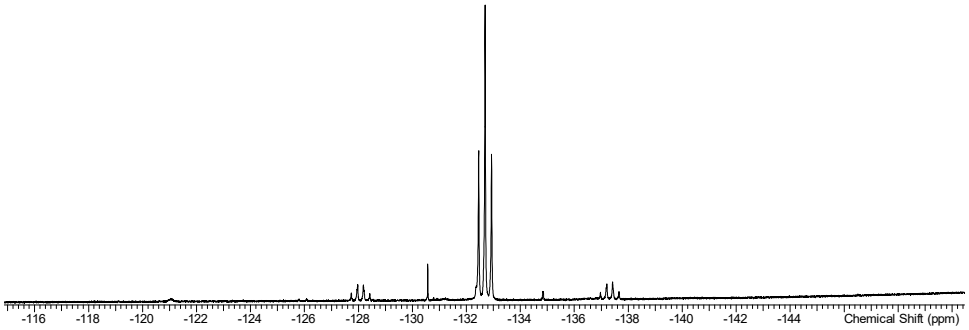

Figure S4.3.1 $^{31}P\{^{1}H\}$ NMR spectrum (CH_2Cl_2, 298 K) ($^{£}[HPMe_3]^{+}$):

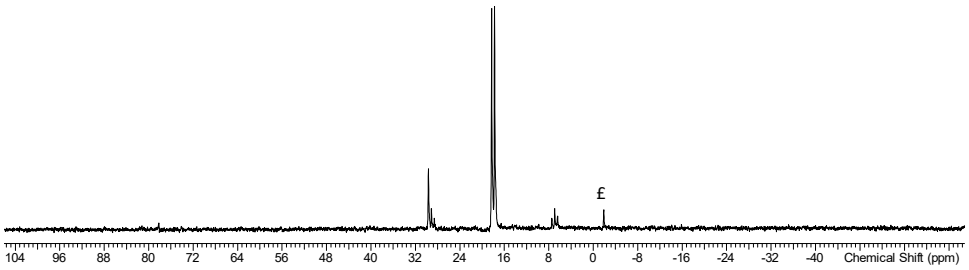

Figure S4.4 ^{119}Sn NMR spectrum (CH_2Cl_2, 183 K):

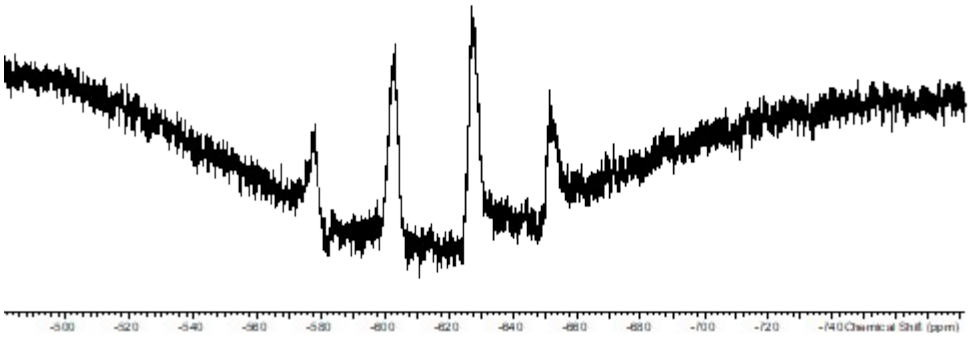

Figure S4.5 IR spectrum (Nujol/cm^{-1}):

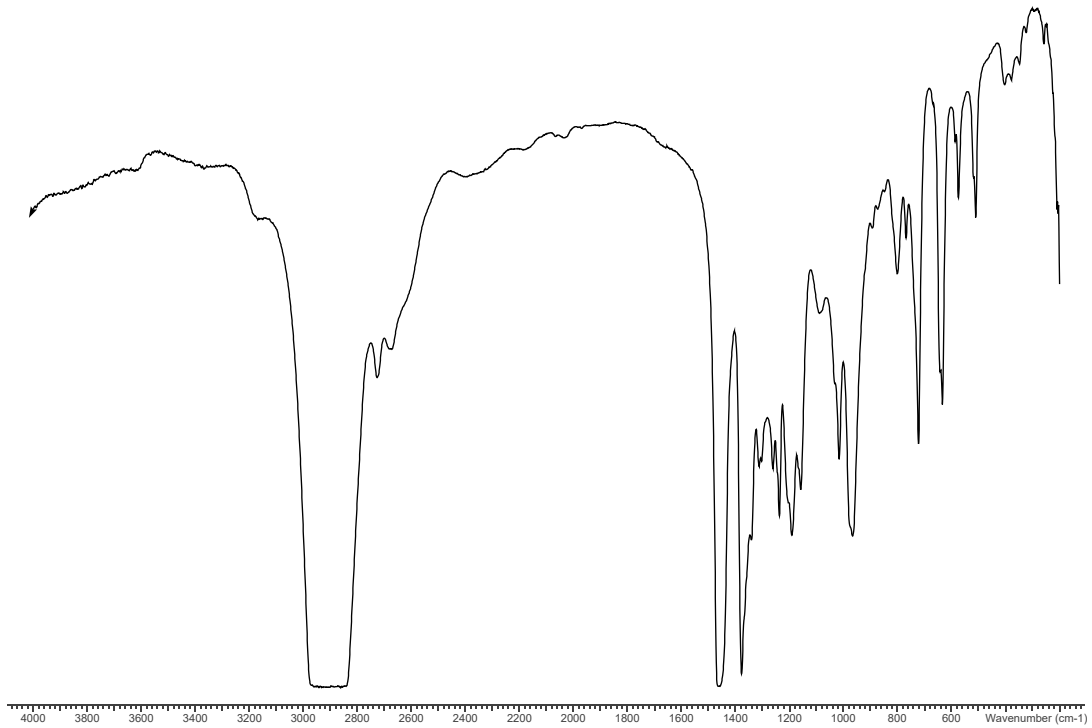

Figure S5 $[SnF_3(P^iPr_3)_2][OTf]$

Figure S5.1 ^1H NMR spectrum CD_2Cl_2, 298 K) (CH_2Cl_2%):

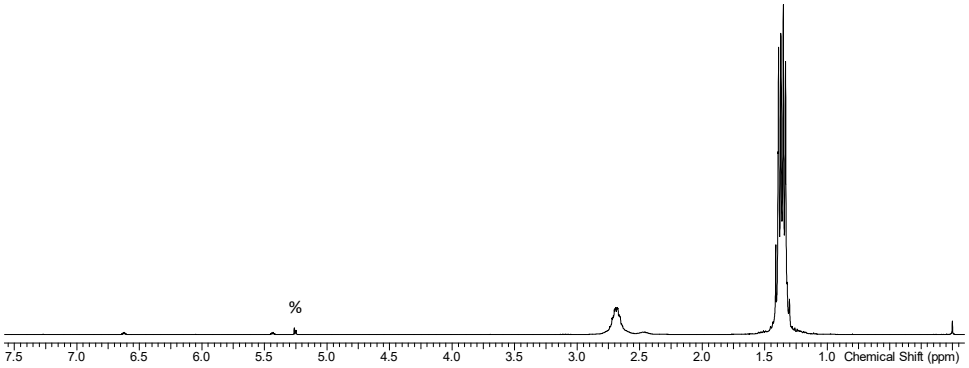

Figure S5.2.1 $^{19}F\{^{1}H\}$ NMR spectrum (CD_2Cl_2, 298 K) (* = $[SnF_4(^{i}Pr_3P)_2]$ impurity; $^{\$}$ = $[FP^{i}Pr_3]^+$ impurity):

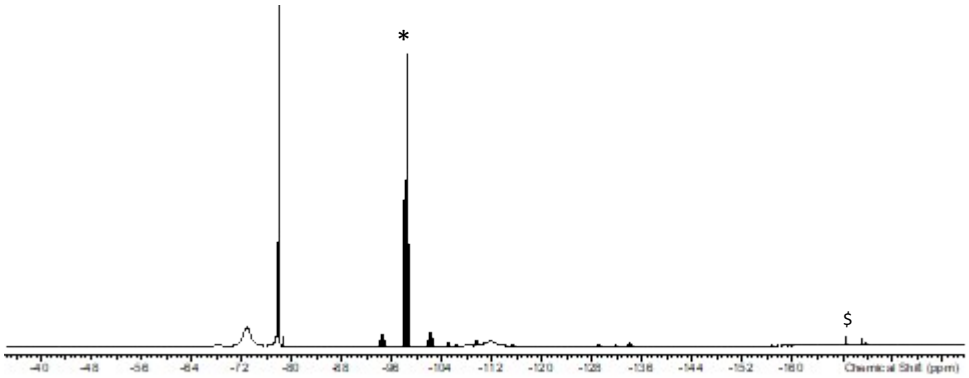

Figure S5.2.2 $^{19}F\{^{1}H\}$ NMR spectrum (CD_2Cl_2, 183 K):

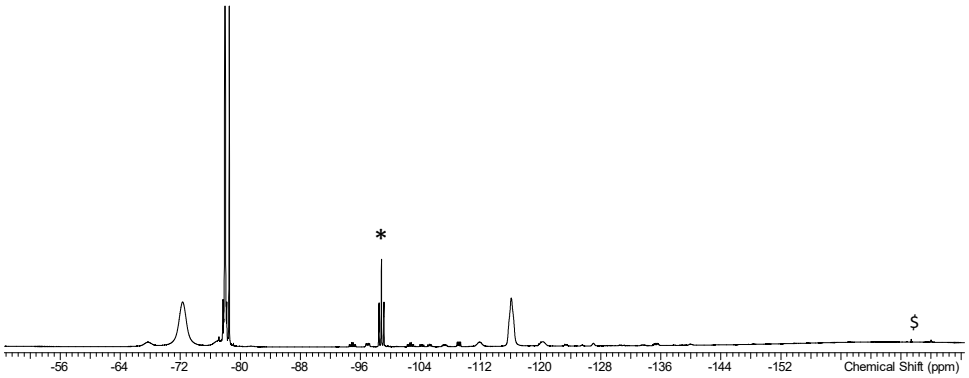

Figure S5.3 $^{31}P\{^{1}H\}$ NMR spectrum (CD_2Cl_2, 298 K) (* = $[HP^{i}Pr_3]^+$ impurity; $^{\$}$ = $[SnF_4(^{i}Pr_3P)_2]$ impurity):

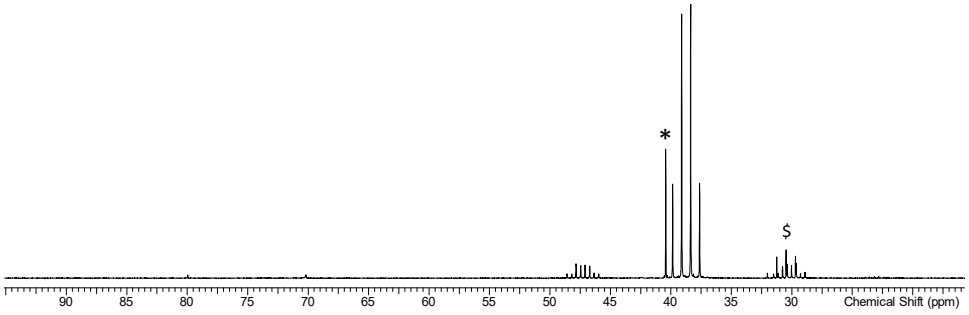

Figure S5.4 ^{119}Sn NMR spectrum (CD_2Cl_2, 183 K):

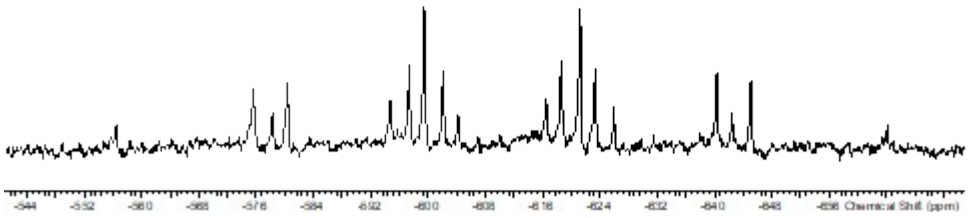

Figure S5.5 Simulated ^{119}Sn spectrum

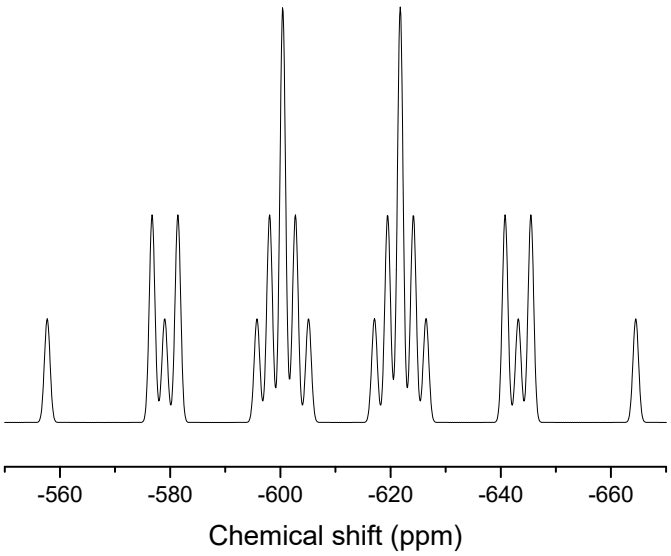

Figure S5.5 IR spectrum (Nujol/cm^{-1}):

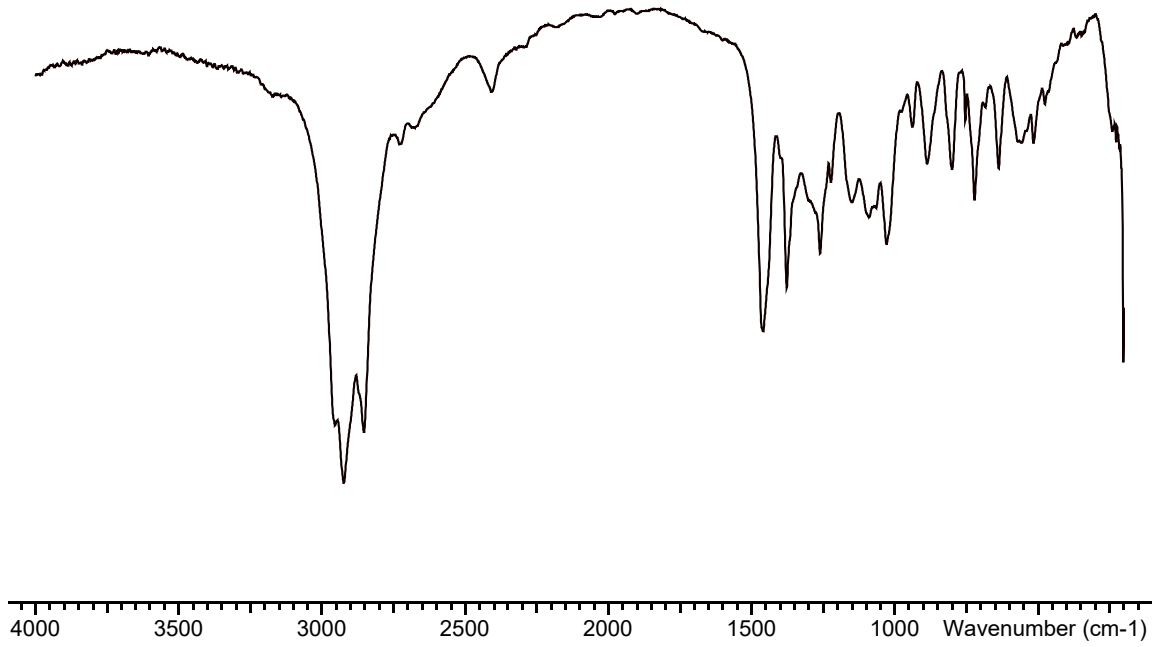

Figure S6 $[SnF_2(^iPr_3P)_2][OTf]_2$

Figure S6.1.1 ^1H NMR spectrum (CD_2Cl_2, 298 K) (*in situ*):

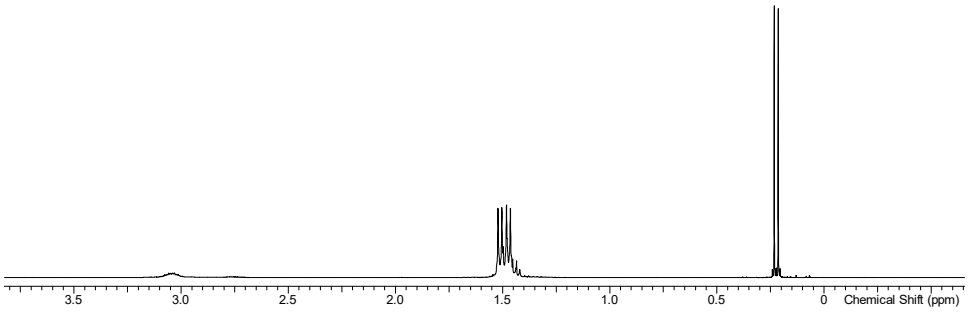

Figure S6.1.2 ^1H NMR spectrum (CD_2Cl_2, 298 K) (isolated complex) (*$[SnF_3(P^iPr_3)_2(OTf)]$, CH_2Cl_2%):

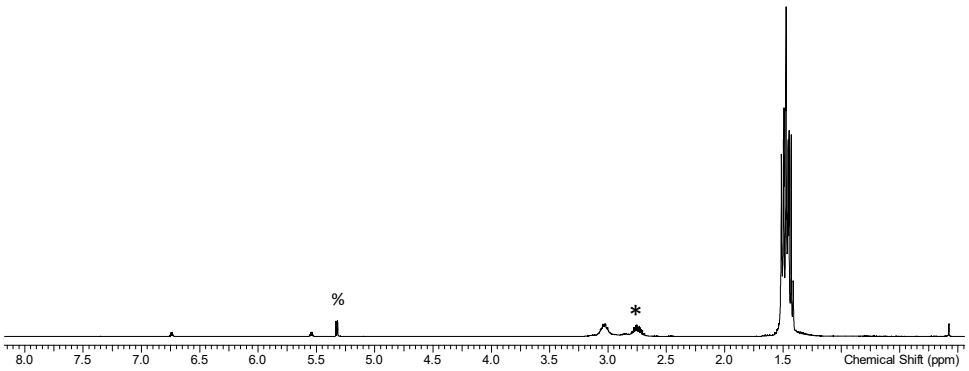

Figure S6.2. $^{19}F\{^{1}H\}$ NMR spectrum (CD_2Cl_2, 298 K):

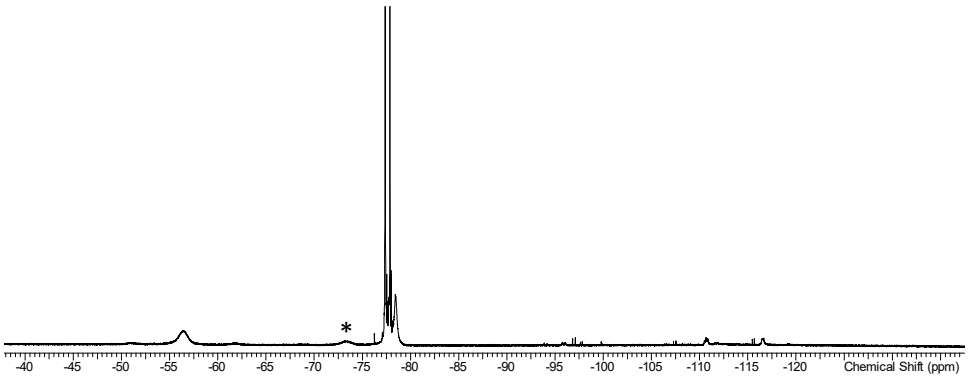

Figure S6.3.1 $^{31}P\{^{1}H\}$ NMR spectrum (*in situ*) (CH_2Cl_2, 298 K) ($^{\$}$ $[H^{i}Pr_3P]^{+}$, * $[SnF_3(^{i}Pr_3P)_2(OTf)]$):

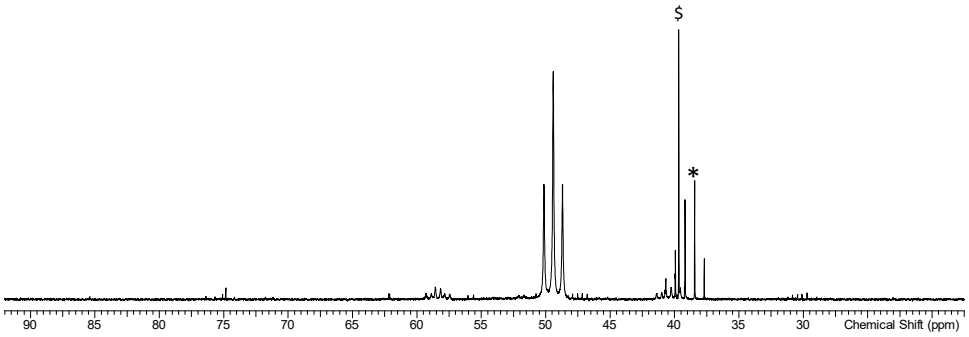

Figure S6.3.2 $^{31}P\{^{1}H\}$ NMR spectrum (CH_2Cl_2, 298 K) (isolated complex) ($^{\$}$ $[H^{i}Pr_3P]^{+}$, * $[SnF_4(^{i}Pr_3P)_2]$):

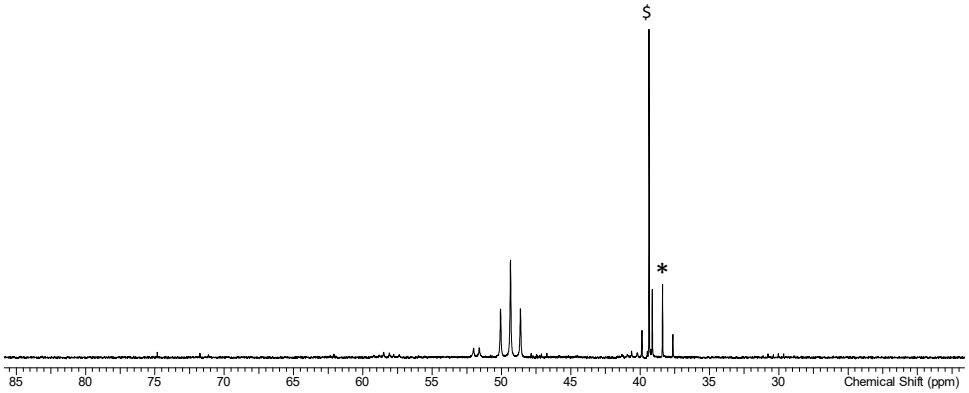

Figure S6.4 ^{119}Sn NMR spectrum (CH_2Cl_2, 183 K) showing a mixture of mono- and bis-triflate complexes

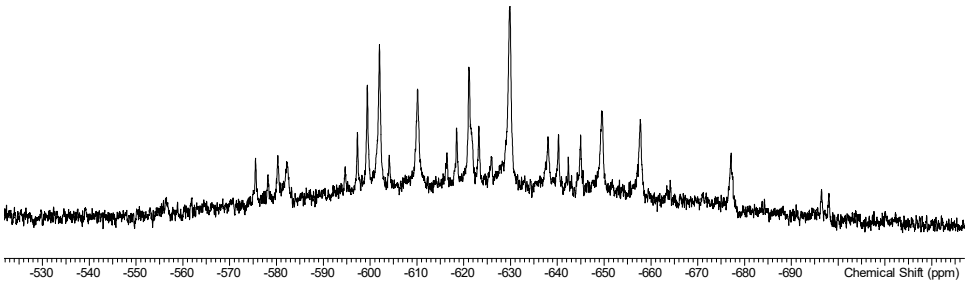

Figure S6.5 IR spectrum (Nujol/cm^{-1}):

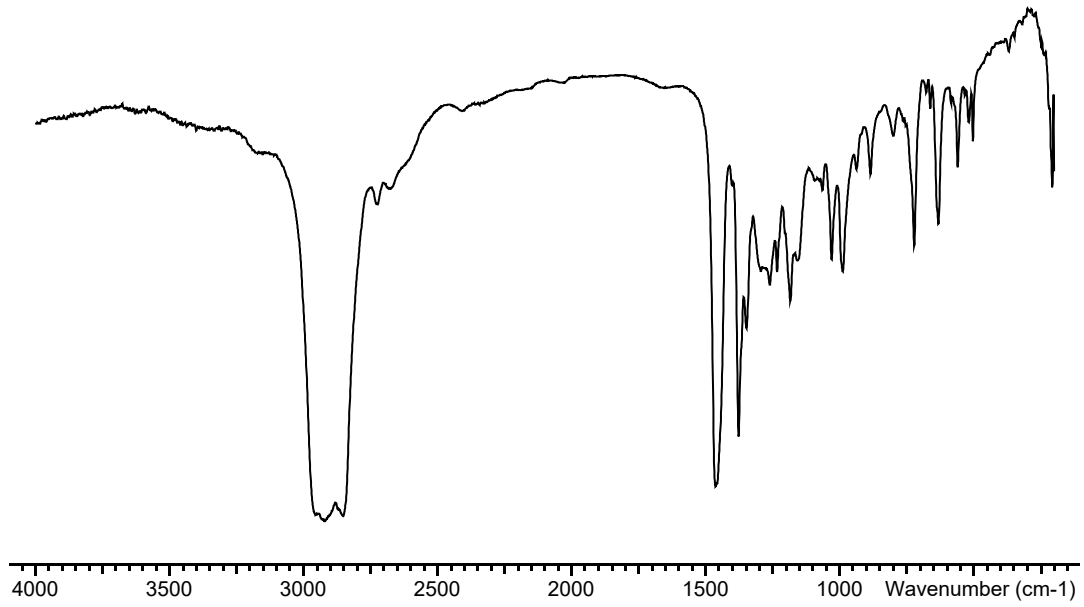

Figure S7 [SnF_4(triphos)]

Figure S7.1 ^{1}H NMR spectrum (CD_2Cl_2, 298 K) (CH_2Cl_2[%]):

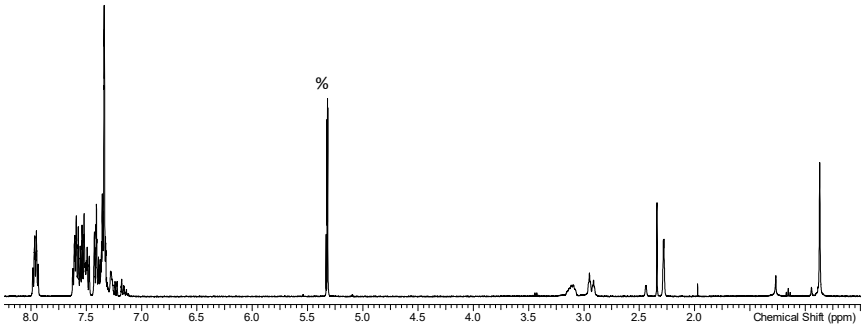

Figure S7.2.1 $^{19}F\{^{1}H\}$ NMR spectrum (CD_2Cl_2, 298 K):

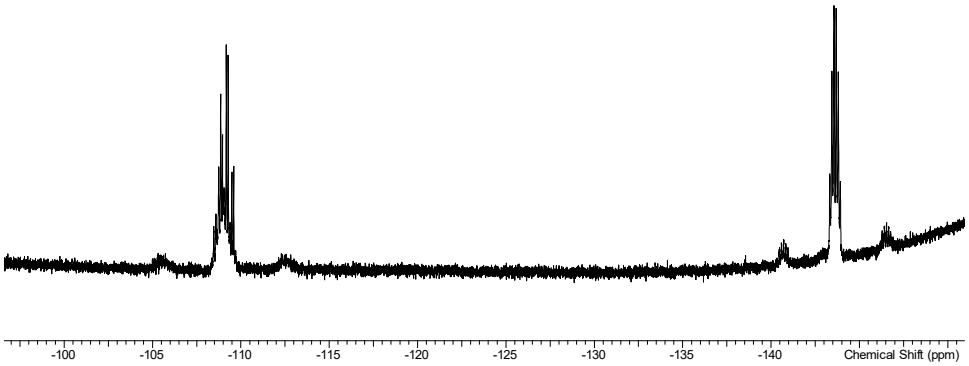

Figure S7.2.2 Expansion of multiplet at -144.2 ppm:

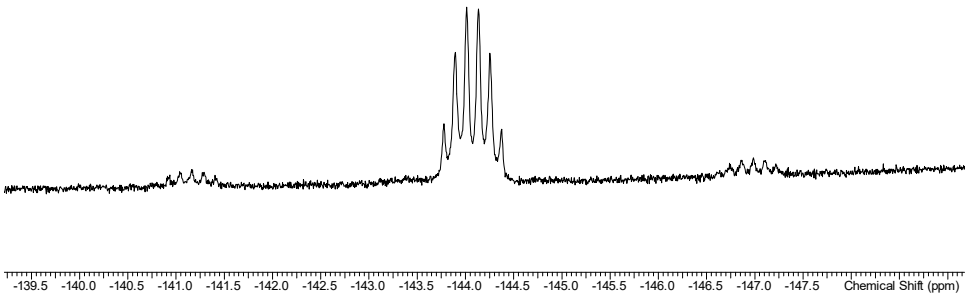

Figure S7.2.3 Expansion of multiplet at -109.7 ppm:

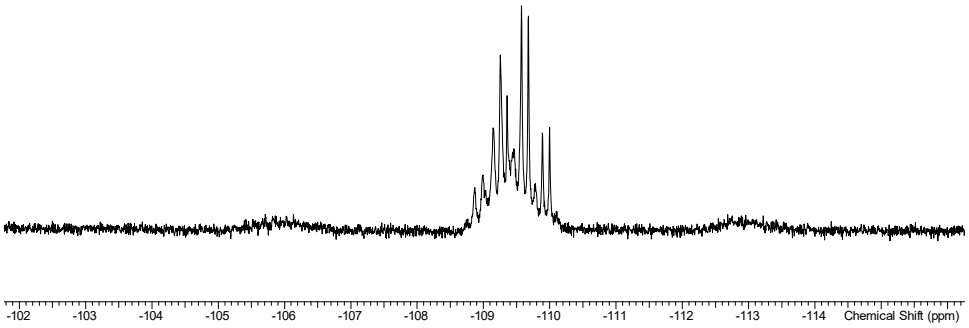

Figure S7.3 $^{31}P\{^{1}H\}$ NMR spectrum (CH_2Cl_2, 298 K) (* = triphos):

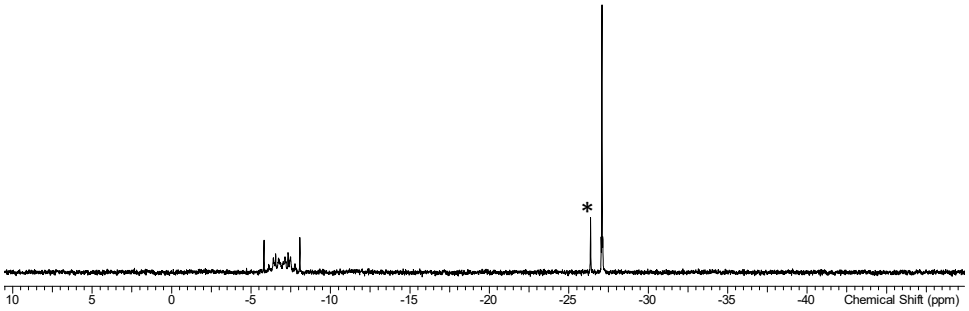

Figure S7.4 ^{119}Sn NMR spectrum (CH_2Cl_2, 183 K):

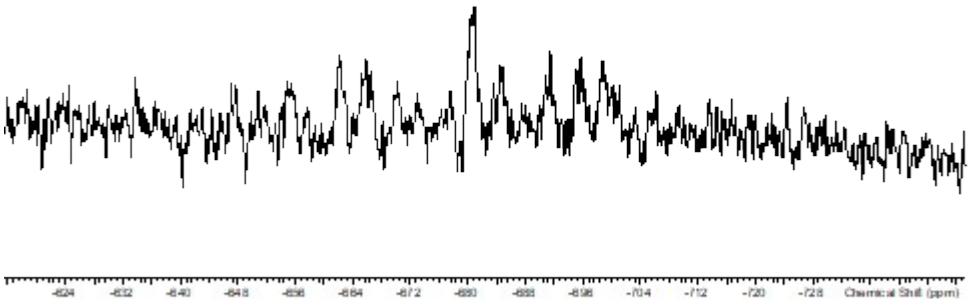

Figure S7.5 IR spectrum (Nujol/cm^{-1}):

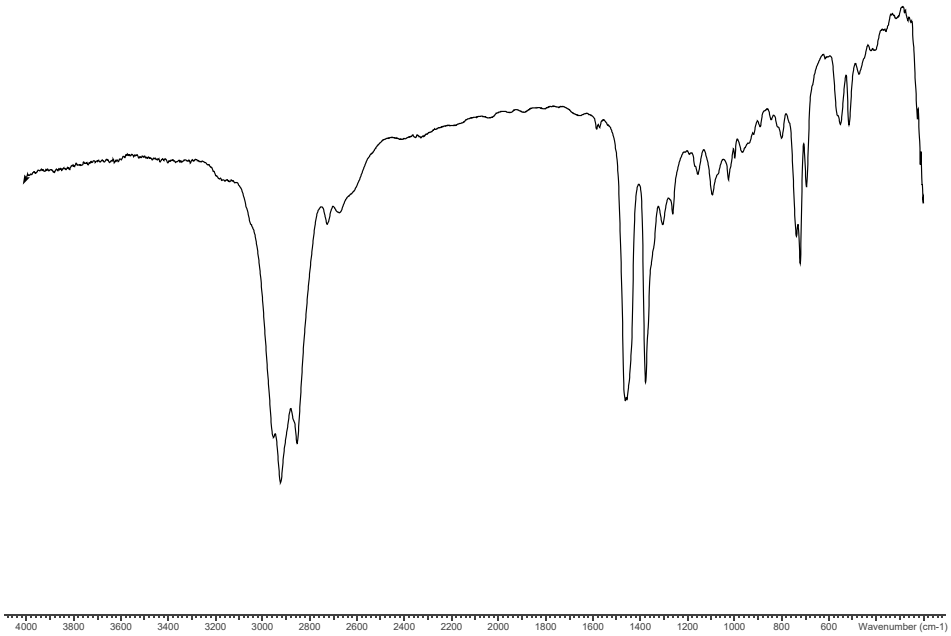

Figure 8 [$SnF_4(dmso))_2$]

Figure S8.1 ^{1}H NMR spectrum (CD_3NO_2, 298 K) (* $MeNO_2$):

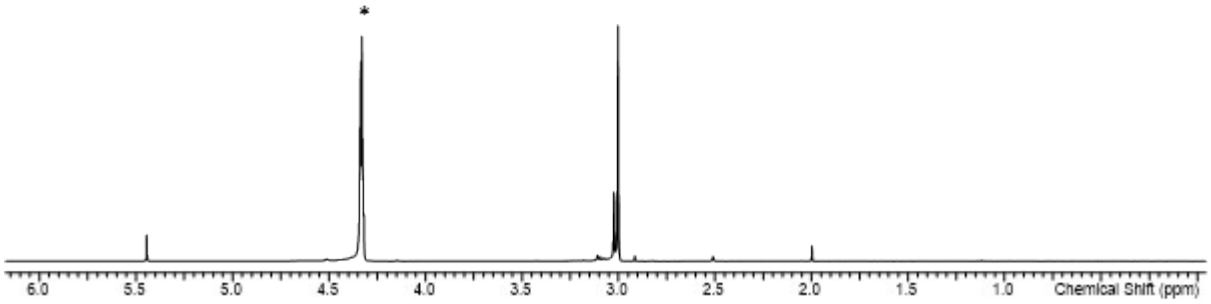

Figure S8.2 $^{19}F\{^{1}H\}$ NMR spectrum (CD_3NO_2, 298 K):

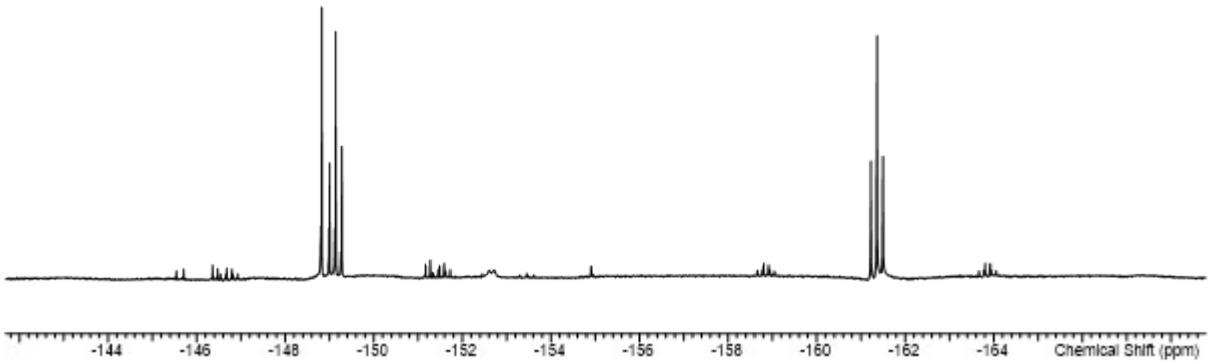

Figure S8.3 ^{119}Sn NMR spectrum (CH_3NO_2, 253 K):

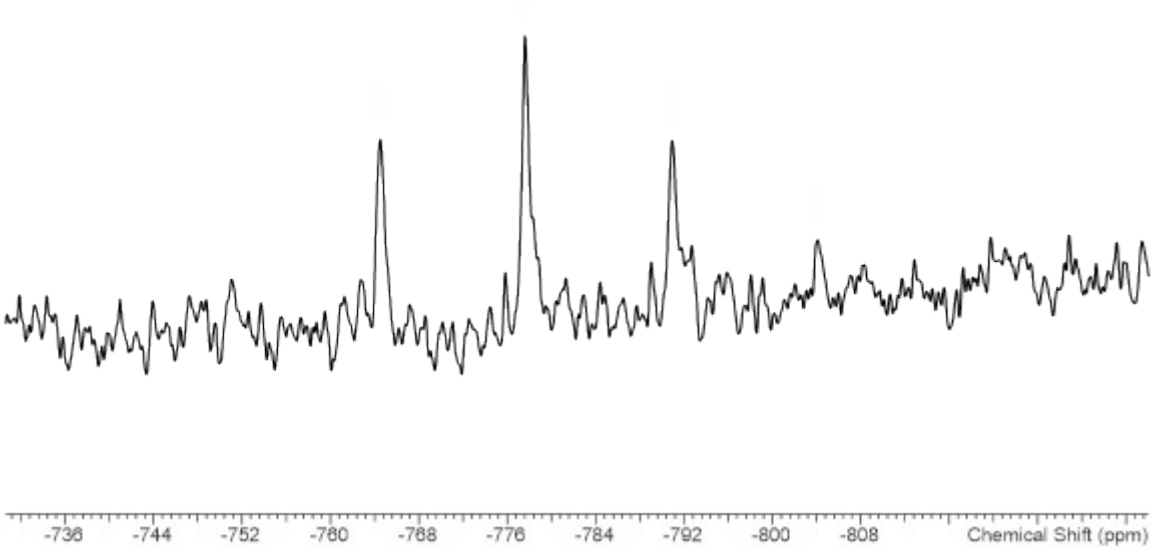

Figure S8.4 IR spectrum (Nujol/cm^{-1}):

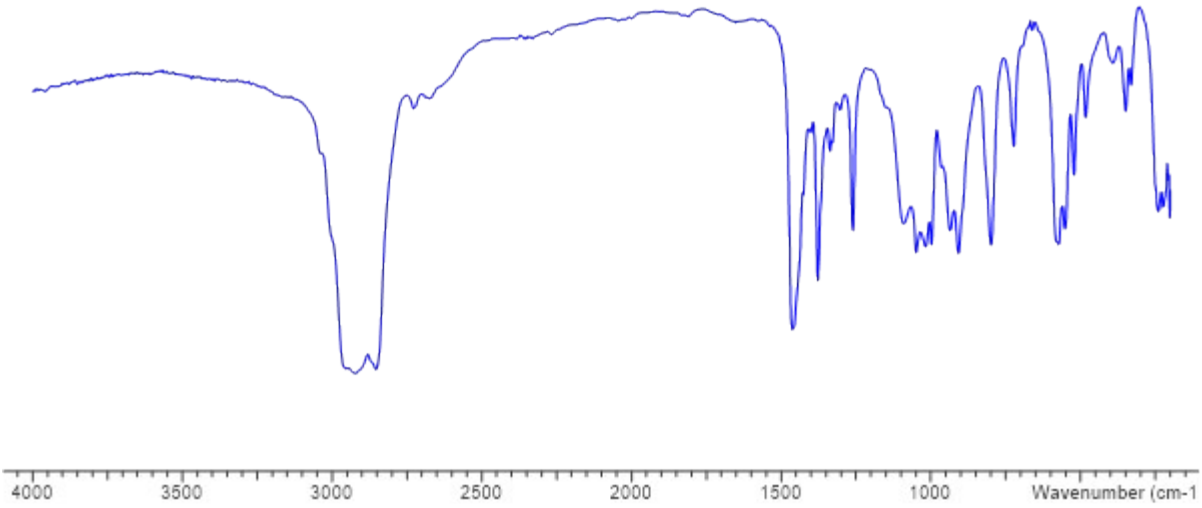

Figure S9 $[SnF_3(dmso)_3][OTf]$

Figure S9.1 ^{1}H NMR spectrum (CD_3NO_2, 298 K) (* $MeNO_2$):

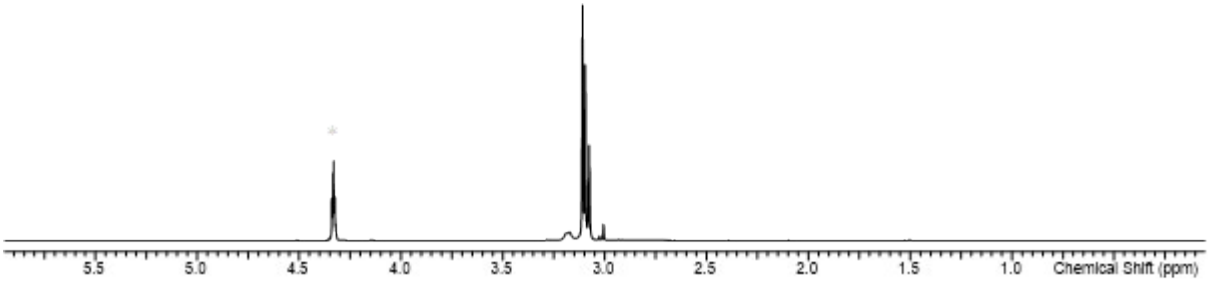

Figure S9.2 $^{19}F\{^{1}H\}$ NMR spectrum (CD_3NO_2, 298 K) (OTf resonance omitted):

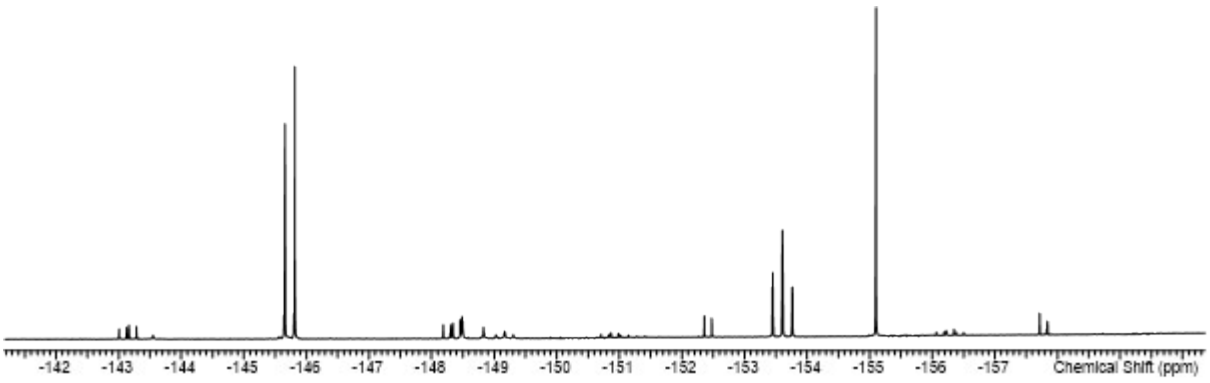

Figure S9.3 ^{119}Sn NMR spectrum (CD_3NO_2, 253 K):

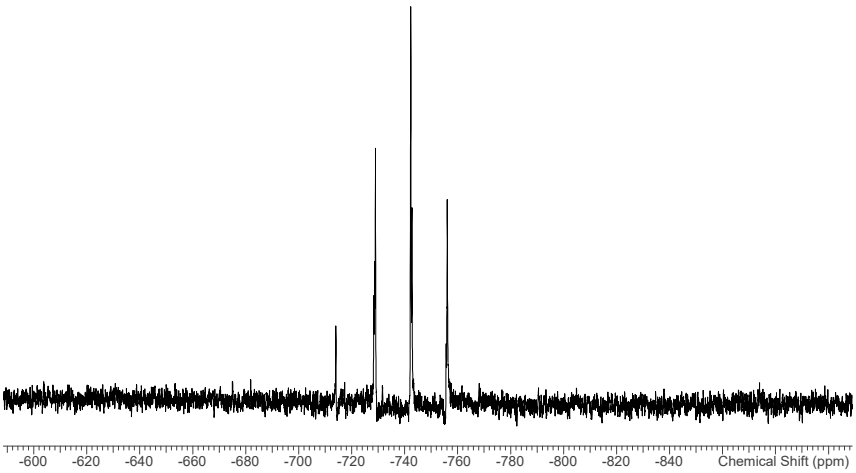

Figure S9.4 IR spectrum (Nujol/cm^{-1}):

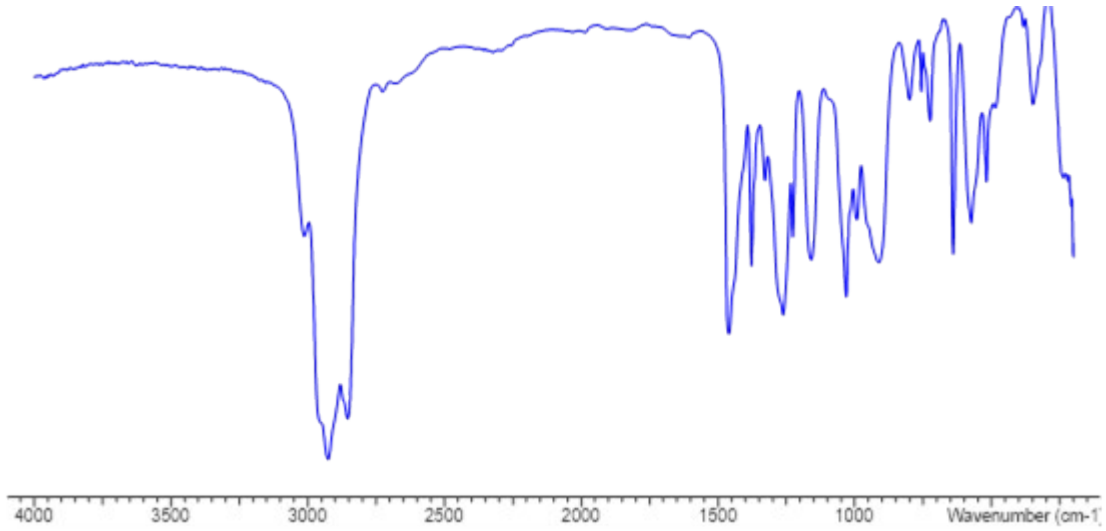

Figure S10 [$SnF_4(DMF)_2$]:

Figure S10.1 ^{1}H NMR spectrum (CD_3NO_2, 298 K) (* $MeNO_2$):

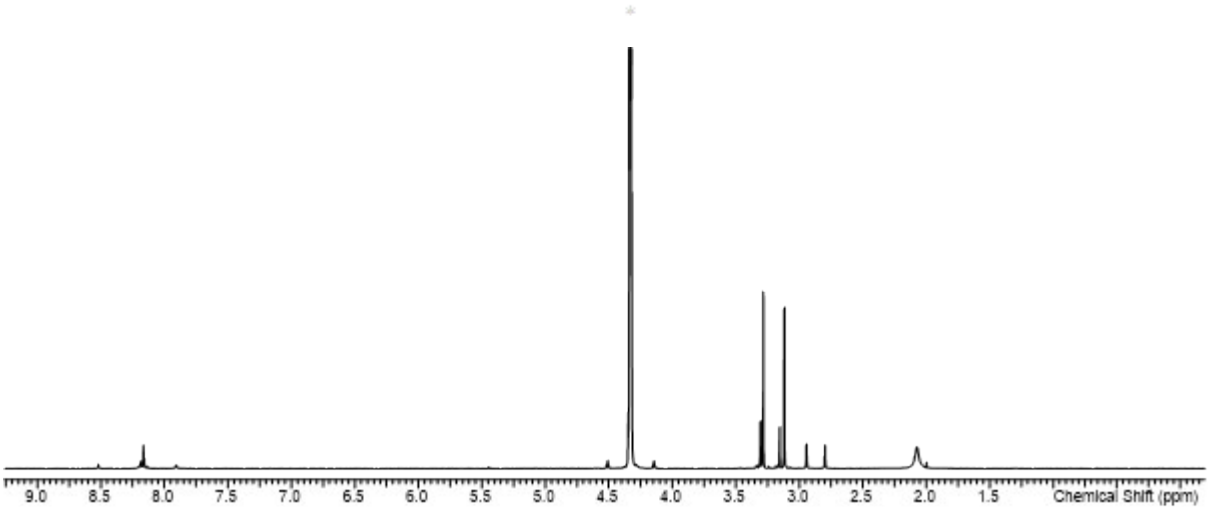

Figure S10.2 $^{19}F\{^{1}H\}$ NMR spectrum (CD_3NO_2, 298 K) (OTf resonance omitted):

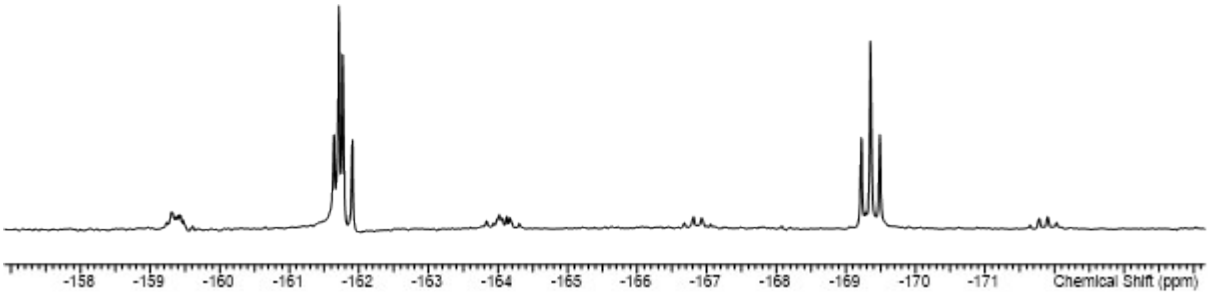

Figure S10.3 IR spectrum (Nujol/cm^{-1}):

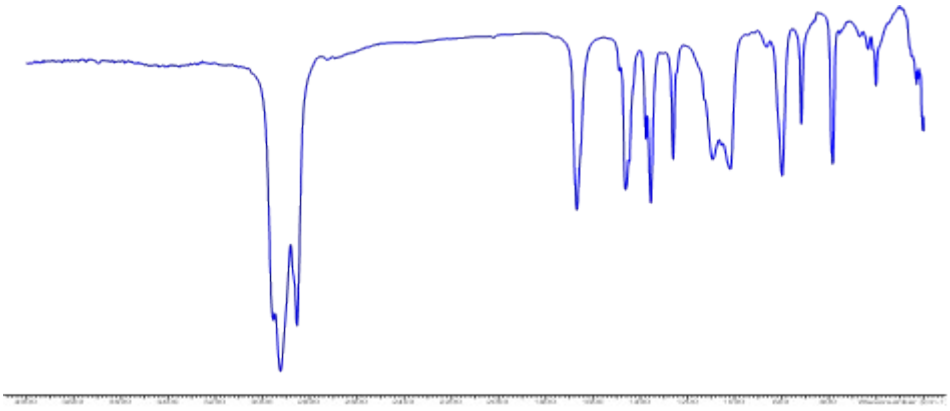

Figure S11 [$SnF_3(DMF)_3$][OTf]

Figure S11.1 ^{1}H NMR spectrum (CD_3NO_2, 298 K) (* $MeNO_2$, $ CH_2Cl_2):

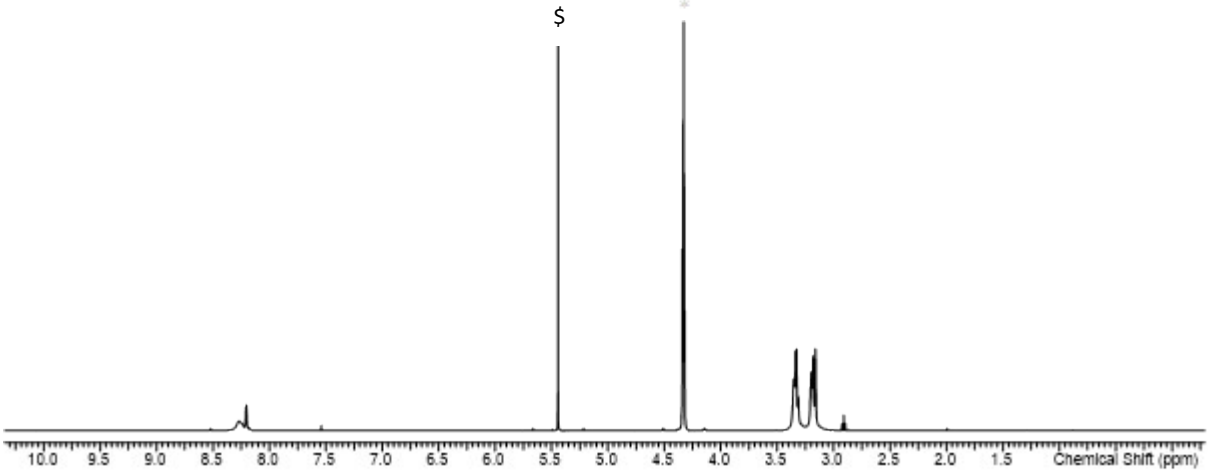

Figure S11.2 $^{19}F\{^{1}H\}$ NMR spectrum (CD_3NO_2, 298 K) (OTf resonance omitted):

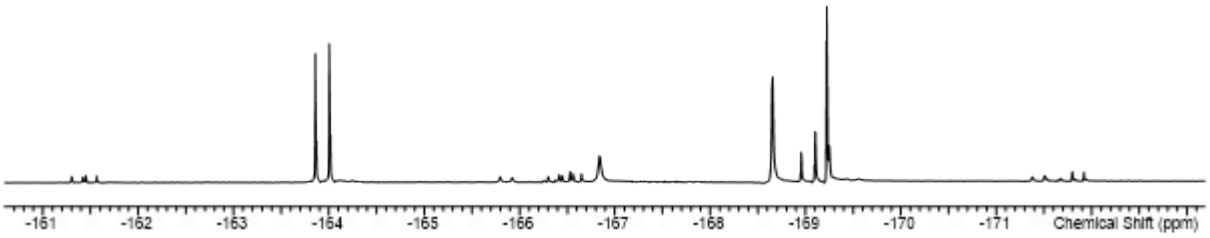

Figure S11.3 IR spectrum (Nujol/cm^{-1}):

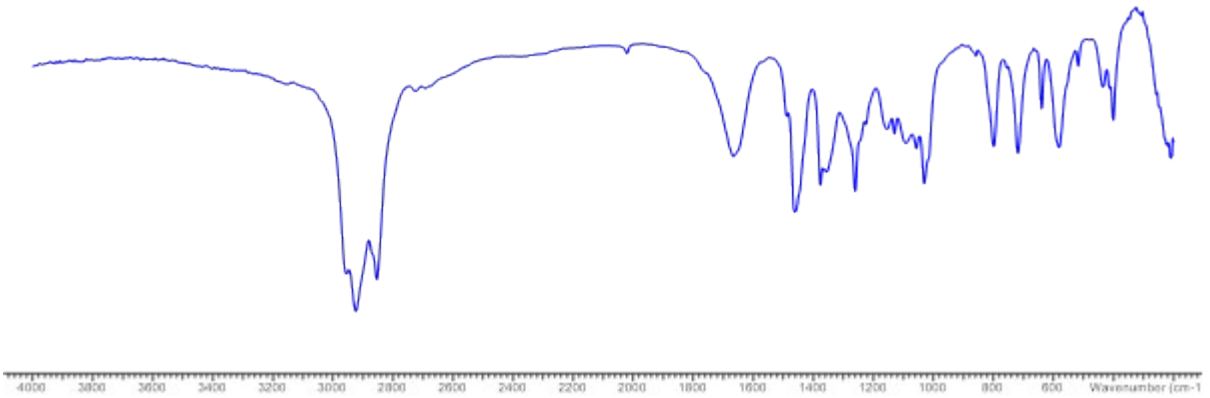

Figure 12 [$SnF_3(py)_3$][OTf]

Figure S12.1 ^{1}H NMR spectrum (CD_3NO_2, 298 K):

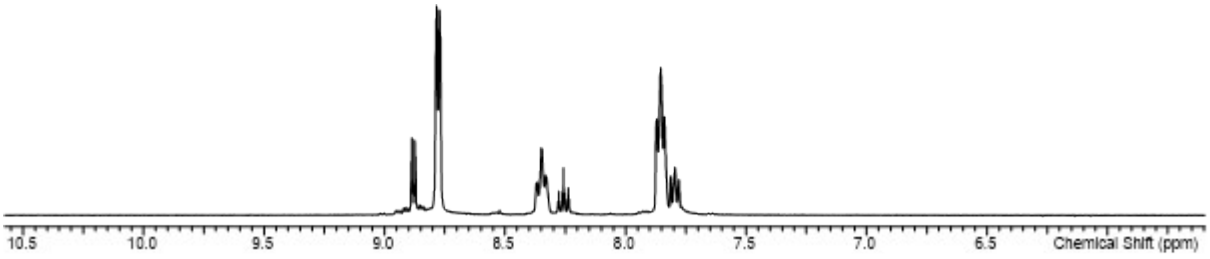

Figure S12.2 $^{19}F\{^{1}H\}$ NMR spectrum (CD_3NO_2, 298 K) (OTf resonance omitted):

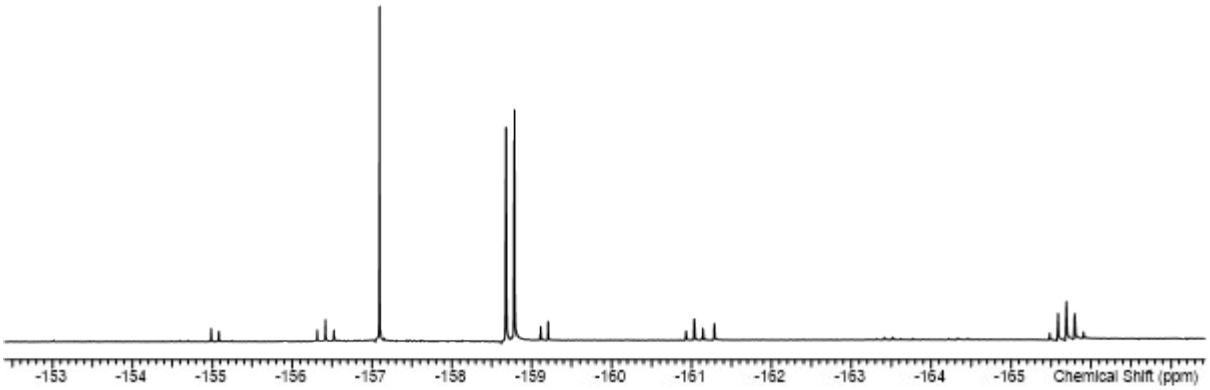

Figure S12.3 IR spectrum (Nujol/cm^{-1}):

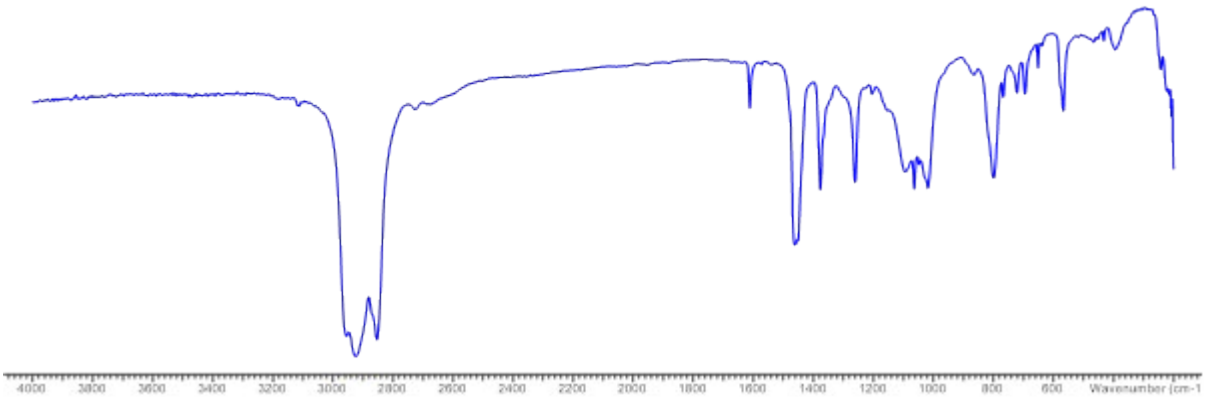

Figure S13 [$SnF_4(pyNO)_2$]

Figure S13.1 ^{1}H NMR spectrum (CD_3NO_2, 298 K):

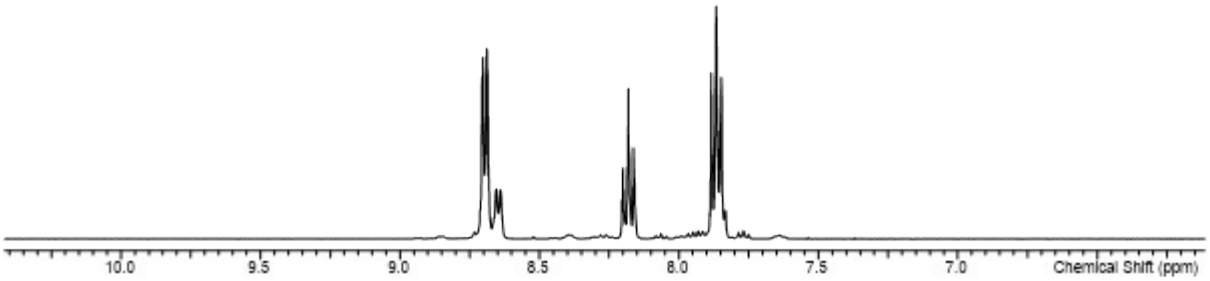

Figure S13.2 $^{19}F\{^{1}H\}$ NMR spectrum (CD_3NO_2, 298 K):

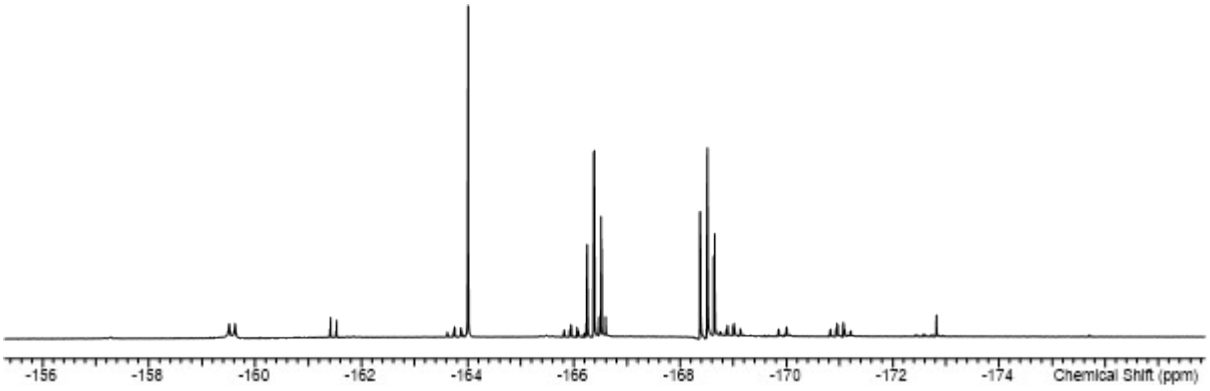

Figure S13.3 ^{119}Sn NMR spectrum (CH_3NO_2, 253 K):

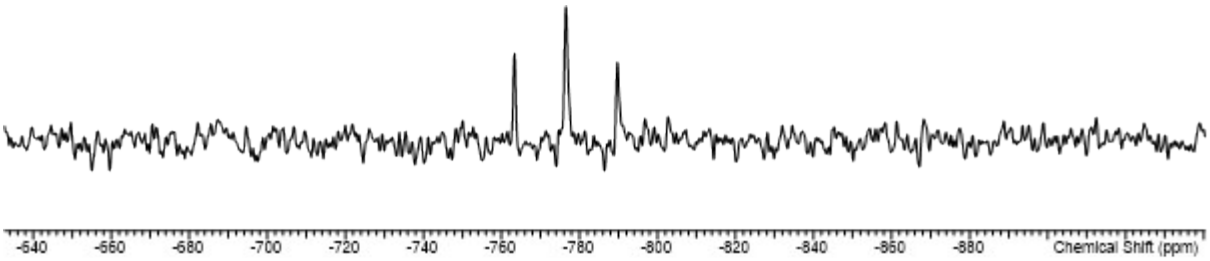

Figure S13.4 IR spectrum (Nujol/cm^{-1}):

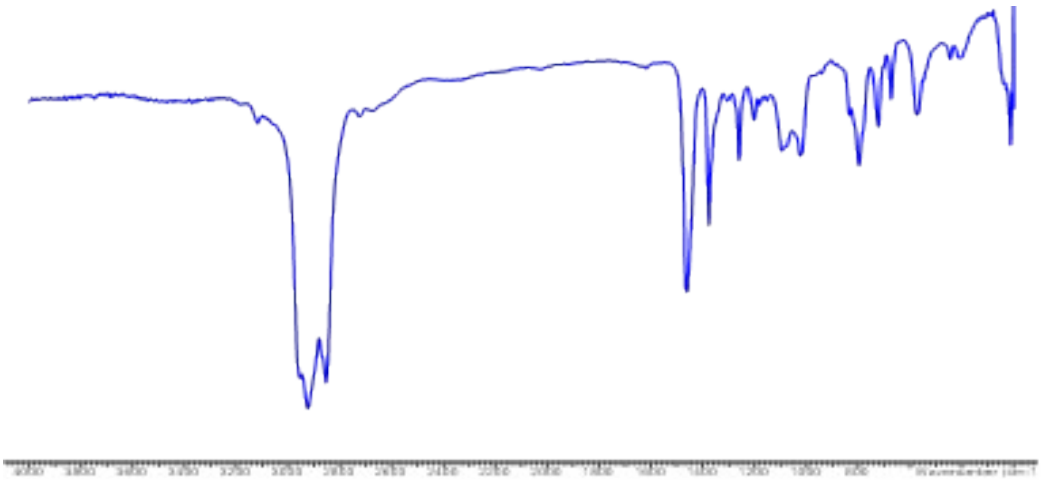

Figure S14 [$SnF_3(pyNO)_3$][OTf]

Figure S14.1 ^{1}H NMR spectrum (CD_3NO_2, 298 K) ($^{\$}$ CH_2Cl_2):

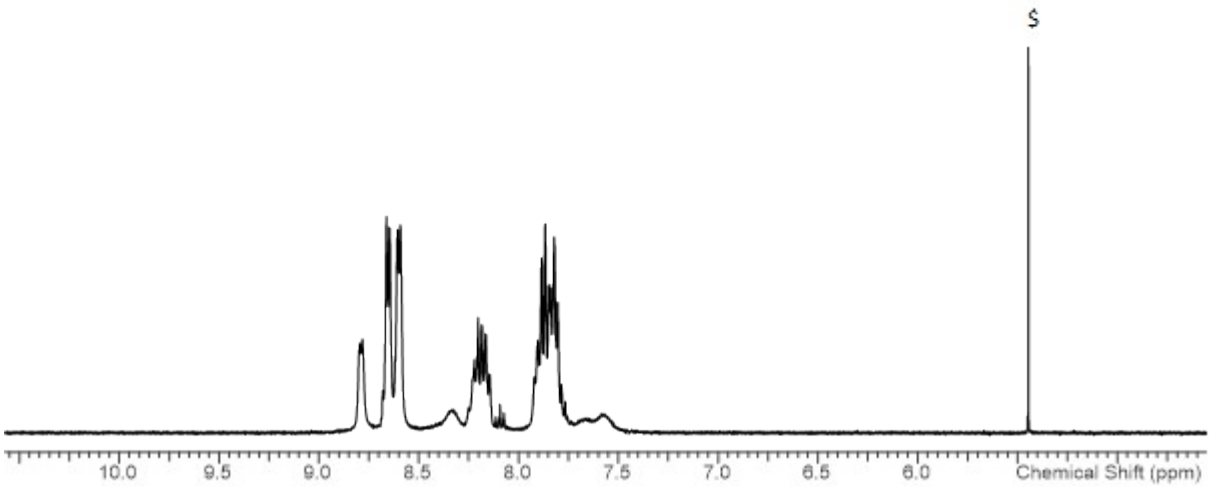

Figure S14.2 $^{19}F\{^{1}H\}$ NMR spectrum (CD_3NO_2, 298 K) (OTf resonance omitted):

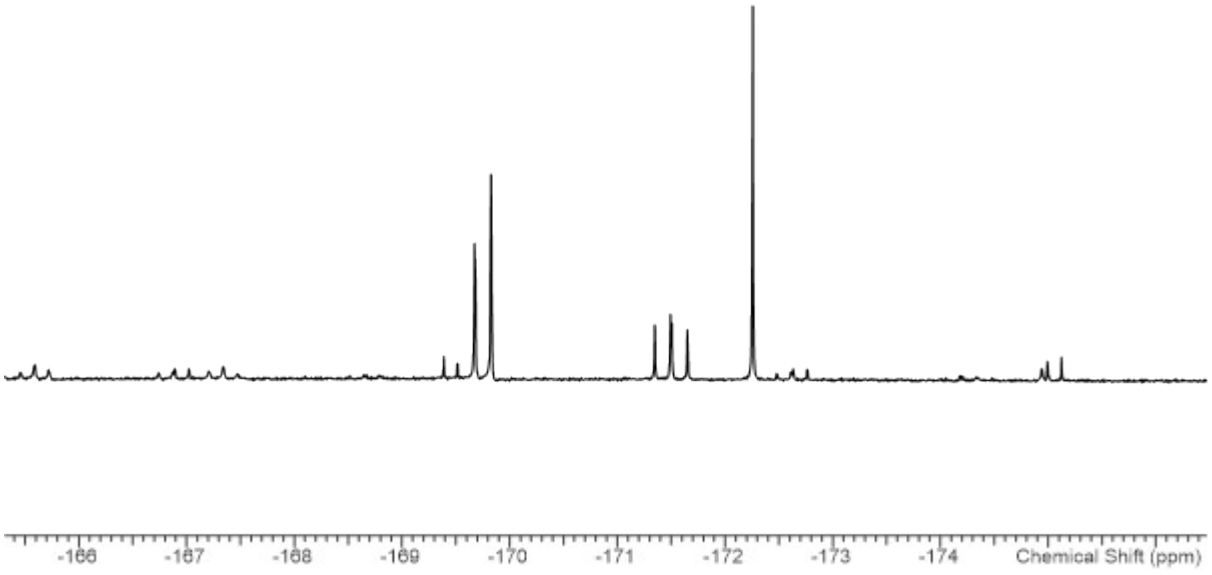

Figure S14.3 ^{119}Sn NMR spectrum (CH_3NO_2, 253 K):

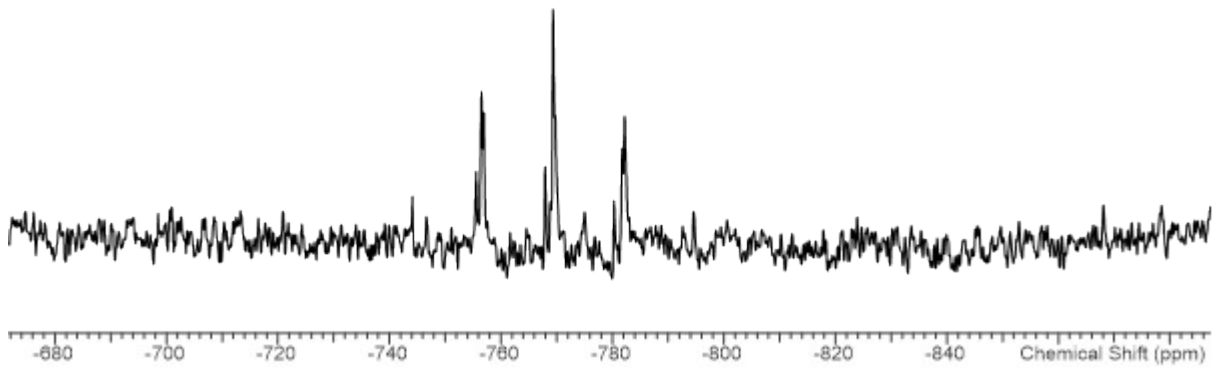

Figure S14.4 IR spectrum (Nujol/cm^{-1}):

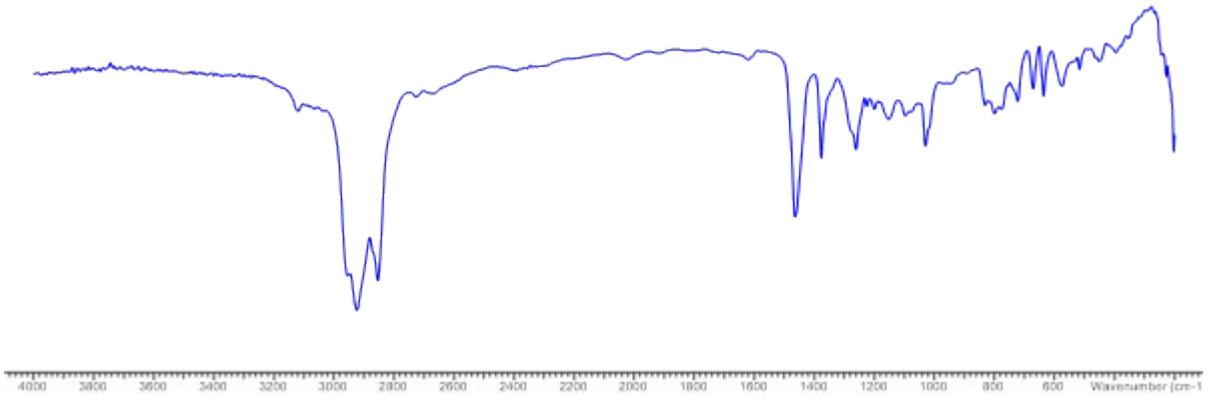

Figure S15 $[SnF_3(OPPh_3)_3][OTf]$:

Figure S15.1 ^{1}H NMR spectrum (CD_2Cl_2, 298 K) (* CD_2Cl_2):

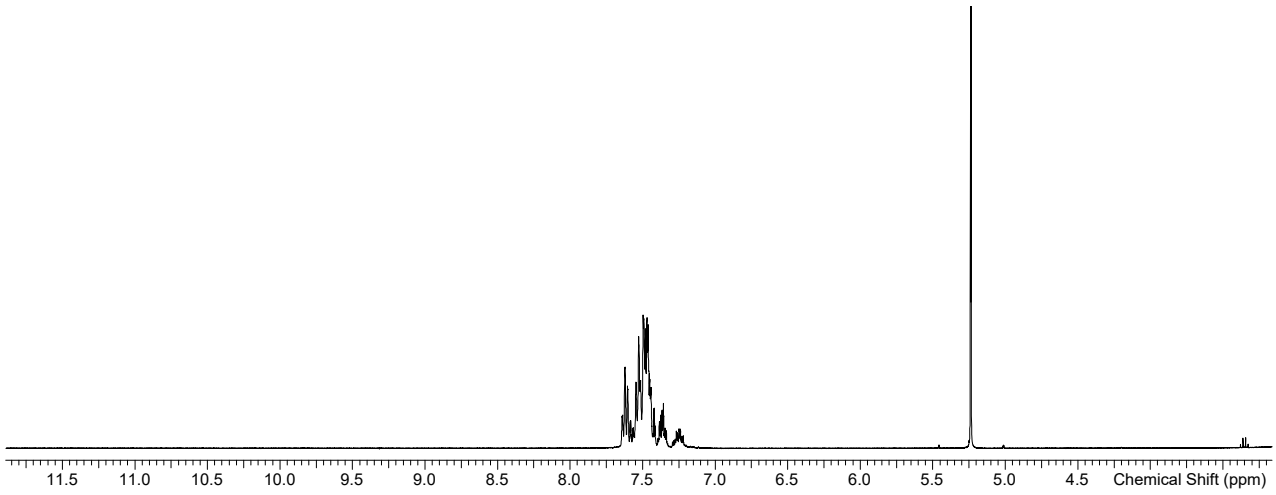

Figure S15.2 $^{19}F\{^{1}H\}$ NMR spectrum (CD_2Cl_2, 298 K) (OTf resonance omitted):

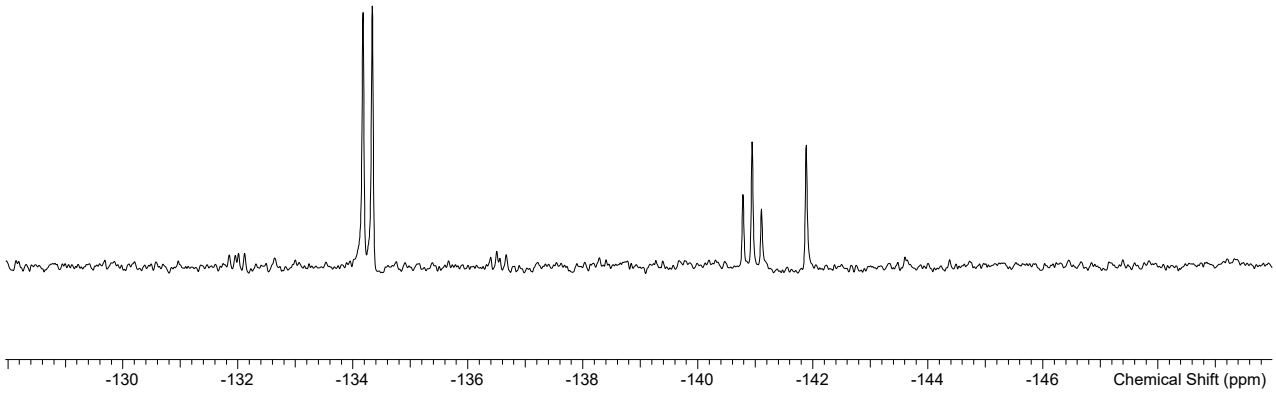

Figure S15.3 $^{31}P\{^{1}H\}$ NMR spectrum (CD_2Cl_2, 298 K):

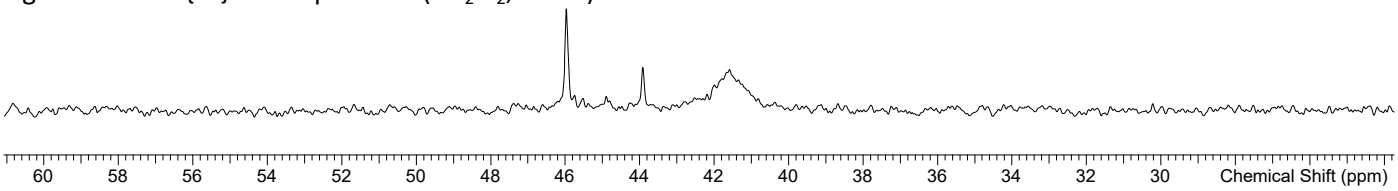

Figure S15.4 IR spectrum (Nujol/cm^{-1}):

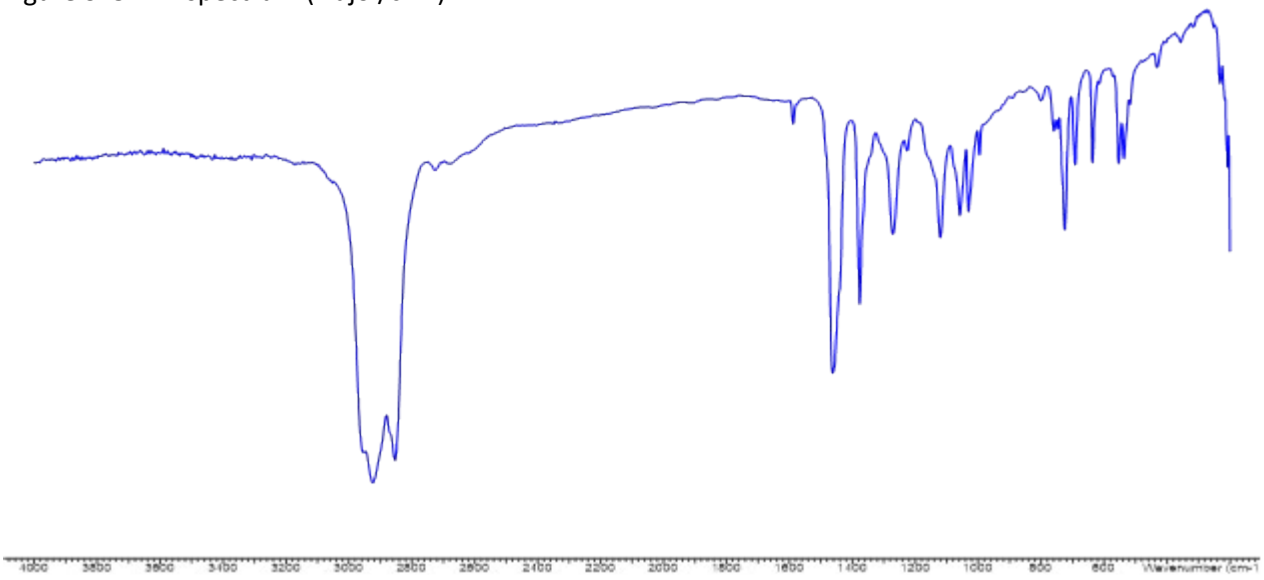

Figure S16 $[SnF_2(OPPh_3)_4][OTf]_2$

Figure S16.1 ^{1}H NMR spectrum (CD_3NO_2, 298 K) ($^{\$}$ CH_2Cl_2, * CD_3NO_2):

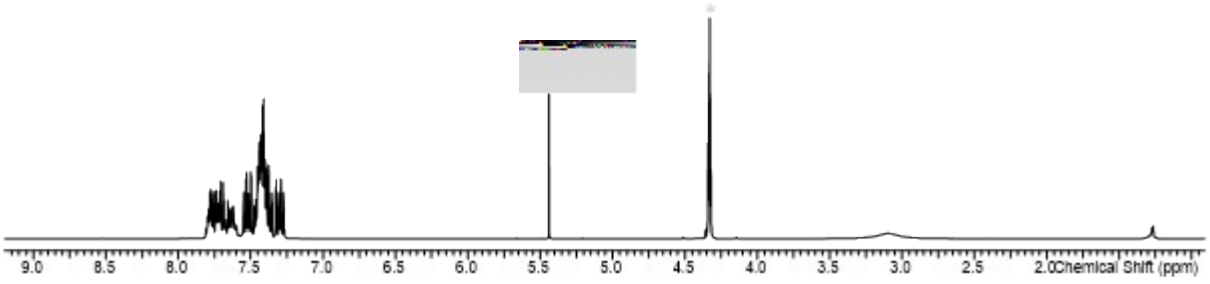

Figure S16.2 $^{19}F\{^{1}H\}$ NMR spectrum (CD_3NO_2, 298 K) (OTf resonance omitted):

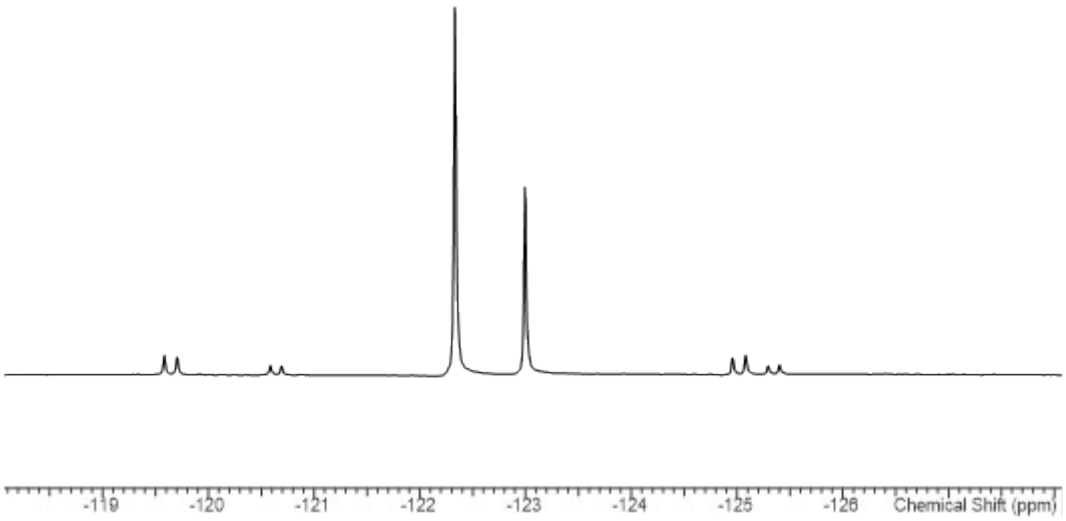

Figure S16.3 $^{31}P\{^{1}H\}$ NMR spectrum (CH_3NO_2, 298 K):

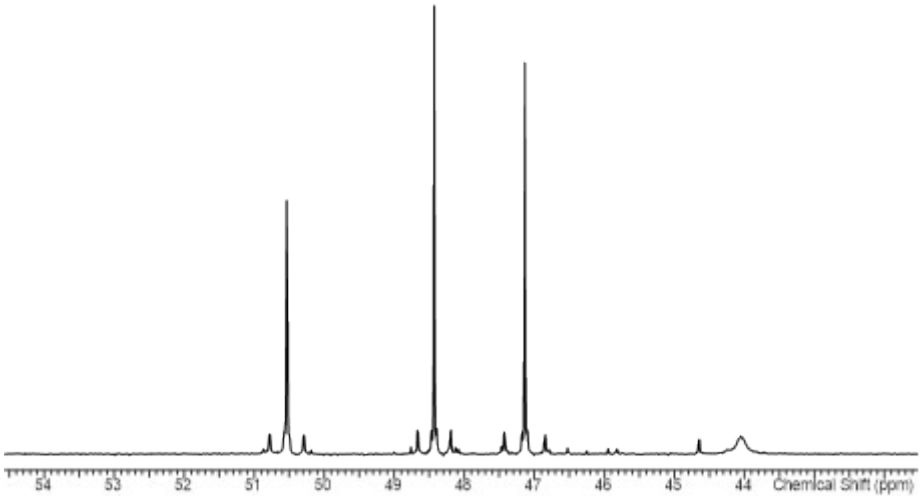

Figure S16.4 IR spectrum (Nujol/cm^{-1}):

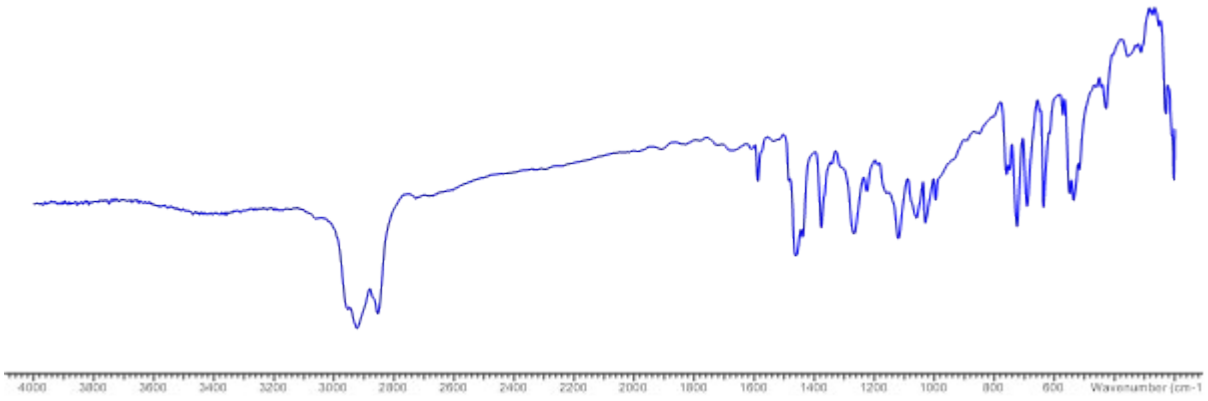

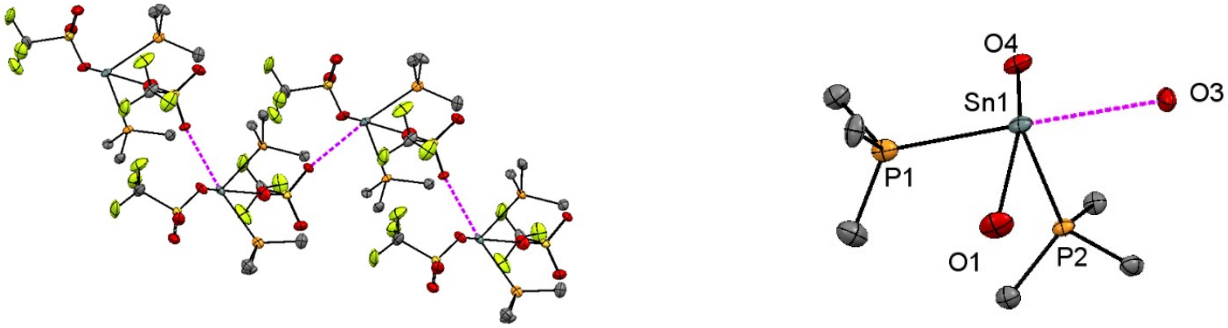

(a) (b)

Figure S17 (a) View of a portion of the extended 1D structure of $[Sn(OTf)_2(PMe_3)_2]$ in the b-direction showing the Sn···OTf contacts (purple dashed lines); (b) the geometry around the tin centre with only the coordinated oxygen from the OTf groups shown.

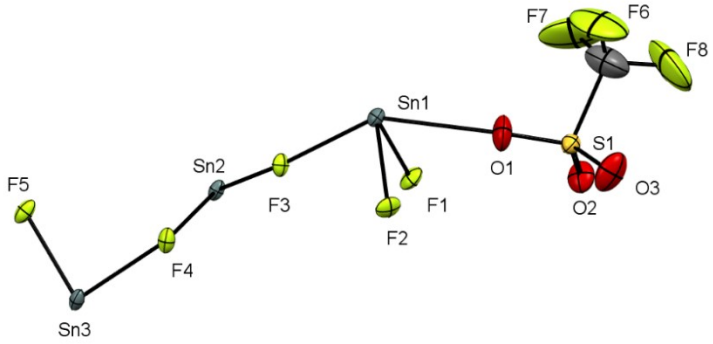

Figure S18 The asymmetric unit of $[Sn_3F_5(OTf)]$ showing the atom labelling scheme. The ellipsoids are draws at the 50% probability level. Selected bond lengths (Å) and angles (°) are: Sn1–F1 = 2.055(2), Sn1–F2 = 2.143(3), Sn1–F3 = 2.148(3), Sn2–F1 = 2.385(2), Sn2–F3 = 2.165(2), Sn2–F4 = 2.175(3), Sn2–F5 = 2.268 (2), Sn3–F2 = 2.183(3), Sn3–F4 = 2.156(3), Sn3–F5 = 2.083(2).